POAC'17
Busan, KOREA

Proceedings of the 24th International Conference on
Port and Ocean Engineering under Arctic Conditions
June 11-16, 2017, Busan, Korea

Model Tests with Ships and Offshore Structures in HSVA's Ice Tanks

Karl-Ulrich Evers[1]

[1] Arctic Technology Department, Hamburgische Schiffbau-Versuchsanstalt GmbH, Hamburg Ship Model Basin (HSVA), Bramfelder Straße 164, D-22305 Hamburg, Germany

ABSTRACT

There is a long history of conducting experimental tests of the interactions between water or ice and structures. For a century, the private and independent Hamburg Ship Model Basin (HSVA) founded in 1913 has been at the forefront of hydrodynamic research. HSVA operates various test facilities such as: Large Towing Tank, Small Towing Tank, Hydrodynamic Cavitation Tunnel (HYKAT), Arctic Environmental Test Basin (AETB) and Large Ice Model Basin (LIMB). This paper describes the historical development of ice technology in the Hamburg Ship Model Basin (HSVA) with its test facilities Large Ice Model Basin (LIMB) and Arctic Environmental Test Basin (AETB). The procedure of model ice production is shown in detail and the methods for determining the mechanical model properties (flexural strength, crushing strength, elastic modulus, etc.) are described. The simulation of various ice conditions (level ice, brash ice, pancakes, ridges, rubble fields, ice floes, etc.) in which model tests with ice breaking ships and offshore structures are carried out are explained. A selection of different projects is presented to demonstrate the versatility and the complex requirements for the execution of model tests.

KEY WORDS: Ice testing facility; ice model tests; model ice properties; offshore structures; ice breaking ship models.

INTRODUCTION

There is a long history of conducting experimental tests of the interactions between water or ice and structures, from Archimedes, through Leonardo da Vinci to the great 19th century pioneers such as Froude and Reynolds. The 20th century saw the development of many of the great hydrodynamics laboratories that remain in use to this day.
For a century, the private and independent Hamburg Ship Model Basin (HSVA) founded in 1913 has been at the forefront of hydrodynamic research. HSVA has influenced and led developments of testing technology, methods, standardisation and numerical procedures to solve complex problems.
HSVA operates various test facilities such as: Large Towing Tank, Small Towing Tank, Hydrodynamic Cavitation Tunnel (HYKAT), Arctic Environmental Test Basin (AETB), Large Ice Model Basin (LIMB) and workshops (Figure 1).
HSVA offers the full range of hydrodynamic services for ships and marine structures. From initial design to detailed investigations of propulsion improvement devices, from concept studies to full scale CFD predictions, all can be done in-house or in close collaboration with

our partners. Model testing with scaled models are still irreplaceable to demonstrate the behavior and the performance of ships and offshore structures, both in open water and in ice covered waters.

This paper gives an overview of the ice testing facilities at HSVA and the production of the model ice, the determination of its mechanical properties are discussed. Selected projects with ships and offshore structures in ice are described.

Figure 1. Oblique aerial view of HSVA's facilities

In 1972 an ice tank was built at HSVA, which with a length of 30 m, a width of 6 m and a depth of 1.2 was at that time one of the most modern in the world. First, sodium chloride and later urea was used as a dopant. These sodium chloride and urea solutions, together with scaled down ice crystals, made it possible to scale the properties of the model ice (e.g. bending strength, compressive strength, and elasticity) corresponding to Froude and Cauchy (Valanto and Schwarz, 1999).

Advanced model testing techniques (e.g. self-propelled ice breaking ships, fixed and floating offshore structures, etc.) required a larger ice tank. The Large Ice Model Basin (LIMB) was put ceremoniously into operation in August 1984 during the 7th IAHR Ice Symposium in Hamburg, Germany.

In the new ice tank "LIMB" with a length of 78 m, 10 m width and 2.5 m / 5 m depth (Figure 2 and Figure3) the HSVA model ice has been further developed.

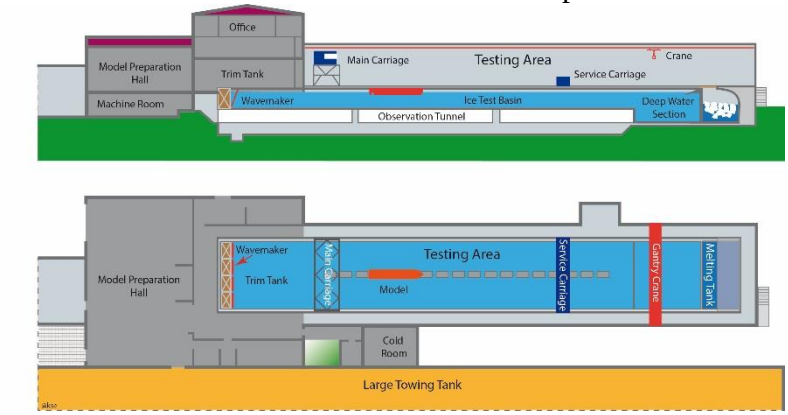

Figure 2. Elevation view (top) and plan view (bottom) of the LIMB.

Figure 3. Large Ice Model Basin (LIMB)

Until late 1980's HSVA has produced a refrigerated model ice grown from an aqueous solution containing urea as a chemical dopant by application of a seeding technique. This type of model ice is strictly columnar structured but has a thin upper granular layer. The brine is entrapped along the boundaries of columnar ice crystals.

Investigations with respect to the improvement of ice properties were made by using various dopants like EG/AD/S and glycerol instead of urea. However, on one hand these chemical dopants reduce the translucence in the water and glycerol is rather costly. The aspect of excellent water translucence is important, because the observation of ice failure processes, propeller-ice interaction and ice clearing by means of underwater video recording. On the other hand the content of sugar in the EG/AD/S dopant may cause bacterial pollution and the chemical stability of the dopant with sugar additive cannot be easily maintained (Timco, 1986; Evers, 2016; Kim and Choi, 2011; Lee, et al. 2010).

Thus, today an aqueous solution containing sodium chloride (~6.8 ppt concentration) is used as dopant at HSVA in combination with air bubble entrapment, in order to get a stable chemical condition in the tank water and to improve the mechanical properties in particular ice brittleness and cracking replication. An air bubble system allows the production of various ice densities. To control ice density and ice porosity the pressure necessary to obtain air saturated water and flow volume is varied (Hellmann, et al.,1992; Evers and Jochmann, 1993).

Transverse carriage

In 2003 the test capabilities in the LIMB were extended. A transverse carriage is permanently installed as a sub-carriage at the rear side of the main carriage. Both carriages together make it possible to run offshore structures or floating vessels in a combined and computer-controlled x-y-motion (planar motion) through the ice sheet. The device gives us the opportunity to simulate, for instance, ice drift scenarios with slow or rapid ice drift direction changes or manoeuvring tests, whereby the model is guided by main carriage and transverse carriage simultaneously while the ice sheet is kept stationary.

The transverse carriage has a maximum static load capacity of 5 kN in any horizontal direction and a load capacity of nearly 10 kN in vertical direction. The horizontal load can be applied on a vertical lever of up to 1.2 m length. A maximum driving force of about 3 kN is applied to the transverse carriage at speeds of up to 0.5 m/s by a geared electric motor (Figure 4).

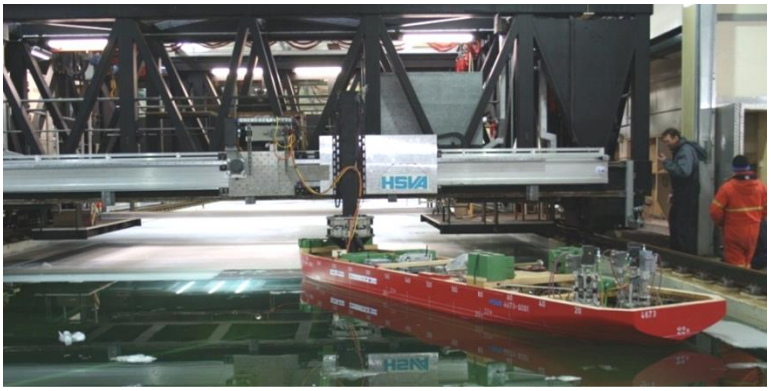

Figure 4. Transverse carriage installed as a sub-carriage on rear side of towing carriage.

For free running tests model and carriage are connected only by the cables, which are needed to transfer electrical power into and the measuring signals out of the model. Cables are kept above the model during manoeuvring operations in order to avoid any force application. The model itself is self-propelled while the rpm of each propeller may be remote controlled by throttles from the carriage. For manoeuvring tests, the rudder or azimuth angle can also be controlled by the operator.
A Qualisys™ motion capture system is used to detect the rigid body motions in all six degrees of freedom (6-DOF). The system uses four cameras installed at the main carriage to detect markers which are located at different positions on the model. Thereby the relative motion between carriage and model are recorded during the free running tests (Figure 5).

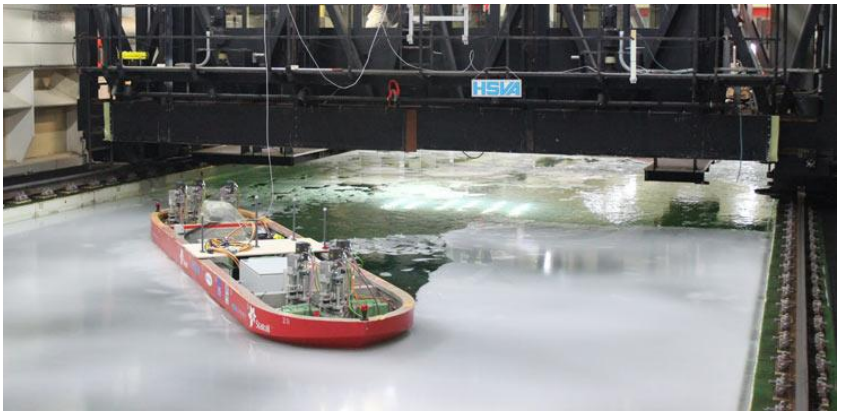

Figure 5. Manoeuvering test of a free running model, model motions in 6-DOF are detected by motion capture system

Removable wave generators

The experiences and results obtained in various projects in the past with “waves in ice” experiments carried out in the Arctic Environmental Test Basin (AETB) have revealed that a larger basin than the AETB is required to perform complex investigations on the behavior of waves in the ice. Therefore HSVA has decided in 2014 to enhance its testing equipment portfolio in the Large Ice Model Basin (LIMB) facility with a wave generator. The system was successfully installed in December 2014. The generator consists of four flap type wave making modules and covers the entire 10 m width of the basin. The flaps of 1.3 m height can be attached to a basement structure such that the hinge position is set 1.2 m above bottom. All

four modules can be installed and removed from the basin within two hours while the basin is filled up with water (Figure 6).

The system is able to produce regular and irregular waves while the maximum wave height is limited to 0.25 m and the maximum deep water wave period is 1.8 seconds with respect to the basin depth of 2.5 m. The system is equipped with an active absorption to reduce reflections. The actual wave signal input is done via user friendly software *AwaSys*™ which transmits the signal to the control software. Figure 7 shows for example the ice floe distribution along the entire basin after wave propagate through an intact ice sheet.

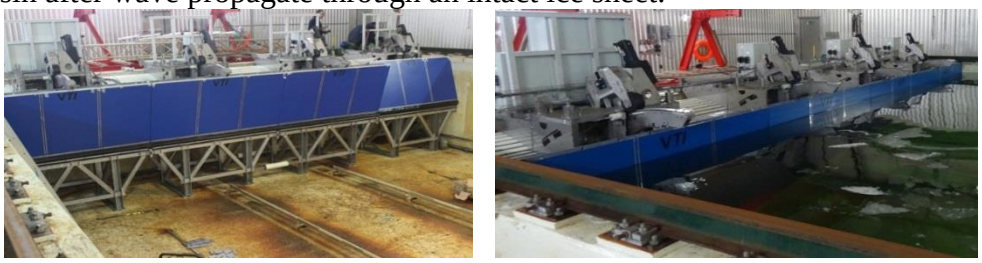

Figure 6. Removable flap type wave generator in Large Ice Model Basin.

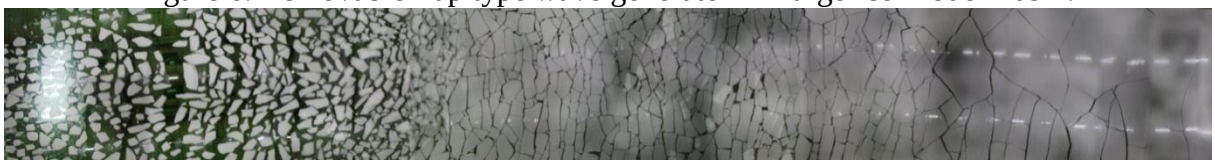

Figure 7. Aerial view of ice floe size distribution along the entire ice tank, the waves propagated from left hand side into undisturbed level ice sheet

Arctic Environmental Test Basin (AETB)

In 1989 after the EXXON VALDEZ oil spill in Prince William Sound, Alaska occurred, the previous "small ice tank" has been renovated and converted to the Arctic Environmental Test Basin (AETB). After the renovation, numerous experiments and investigations were carried out with regard to "oil in ice", testing of mechanical oil recovery systems, geophysical experiments like frazil and pancake formation and research projects in the area of artic marine biology and chemistry.

In this context it is mentioned that since 1996 possibility is given for international research groups to make use of HSVA's ice tanks (LIMB and AETB) for research projects financially supported by the European Union. Young engineers and researchers have carried out numerous projects in these facilities which were financially supported by the European Commission (www.hydralab.eu).

In 2016 the oil-resistant coating of the basin was completely renewed and a movable crane platform was designed and built (Figure 8).

Figure 8. Arctic Environmental Test Basin (AETB) with movable working platforms

MODEL ICE AT HSVA

General

By using a single dopant system the grown model ice sheet consists of a three-layer system:

- thin hard upper granular layer
- transition layer with higher dopant concentration
- weak columnar crystal layer

Figure 9 shows a thin section of first-year sea ice sample taken in the Arctic. The structure of this ice type is columnar with a thin hard granular layer on top. Since the model ice is denser than in full scale , the criteria for buoyancy similitude may not be met. Thus methods were developed at NRC Canada for EG/AD/S CD-ice (Spencer and Timco, 1990) and HSVA, Germany, for sodium chloride doped model ice to incorporate air bubbles (Figure 10) into a growing ice sheet in order to control its overall density (Evers and Jochmann, 1993).

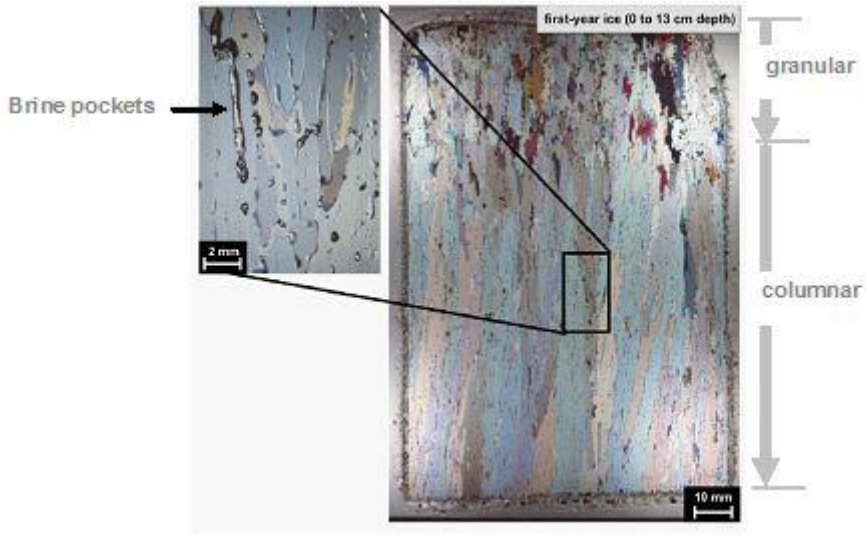

Figure 9. Thin section of first-year ice showing the ice platelets and the brine pockets long the grain boundaries (photo courtesy of M. Johnston; Timco and Weeks, 2010).

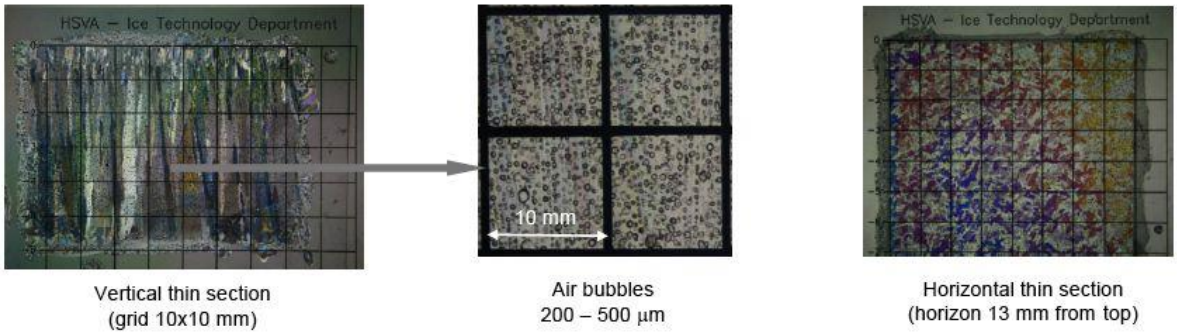

Figure 10. Vertical and horizontal thin sections with micro bubble inclusions in HSVA's model ice.

For this purpose a patented technique (Hellmann, et al.,1992) was developed at HSVA and is applied by pressing air saturated water under high pressure through perforated tubes fixed at the bottom of the ice tank during ice growth process at about – 20°C air temperature. When the water leaves the tubes the pressure drops. Tiny air bubbles of 200-500 µm diameter rise upwards and are embedded in the growing ice sheet. The content of micro bubbles affects also the elasticity/ strength ratio E/σ_f which increases significantly and the ice behaves more brittle when it fails. A secondary effect of air inclusions is the opaque colour of the ice giving a better contrast between model and ice in images taken from underwater (Evers and Jochmann, 1993).

Model ice production technique

The preparation of the ice sheet is started by a seeding procedure. For this purpose fresh water is sprayed under pressure into the cold air of the ice tank (Figure 11). The droplets freeze in the air forming small ice crystals which settle on the cold water surface. By this method the growth of a fine-grained ice of primarily columnar crystal structure is initiated. The water in the tank is fresh water doped with 6.8 ppt salt. After a thin closed icy skin has formed on the surface of the water the ice tank is cooled to -20°C and the ice sheet continues to grow.

During the ice growth continuously air-supersaturated water is discharged in the ice tank through the perforated pipe system fixed at the bottom of the ice tank. As a result of the pressure rundown the air dissolved in water is released and air bubbles rise upward to the top where they are embedded between the growing ice crystals as shown in Figure 10.

This impure ice sheet is inherently softer than pure-water ice but may be harder than the scaled strength desired. Once a desired thickness is achieved, the air temperature is raised to a tempering temperature, in order to weaken the ice according target strength.

As the temperature of the ice rises the dopants come out of frozen solution and form liquid brine pockets. These brine pockets slowly drain out of the ice sheet thus weakening it. The strength of the ice continues to decrease approaching an asymptotic value. This softening is often referred to as "warming-up".

Figure 11. Water is sprayed by means of nozzles under high pressure into the air of the pre-cooled ice tank (left photo) where crystal nuclei are formed which settle down on the water surface (right photo).

Due to the embedded air the model ice fails brittle, i.e. the E/σ_f -ratio increases and the size of broken ice pieces becomes more realistic compared to model ice without air bubble treatment. Another advantage of the air content in the ice is the possibility to adjust the ice density so that the density difference between ice and water is within the natural range (Evers and Jochmann, 1993).

Before reaching the target ice thickness the cooling system is switched off and the air temperature is raised slightly above the freezing point. This temperature is kept until the properly scaled strength is reached. Then, the heat transfer into the tank is reduced to a minimum in order to keep the strength nearly constant for the duration of the test. A typical "freezing-warming cycle" is shown as an example in Figure 12.

In a first step the ice tank is precooled [1]. During the seeding process the cooling process is interrupted and the air temperature rises [2]. When the seeding procedure is finished the cooling process starts again and the air temperature in the ice tank decreases to about –20°C. The duration of cooling depends on the required target ice thickness and has to be finished in due time taking a certain additional ice growth into account [3]. The heating process is initiated by heated air blown into the tank instead of cold air. The tempering of the ice causes a decrease of ice strength. During the tempering ice properties (e.g. ice strength, ice thickness, etc.) at different locations in the ice tank are measured in order to determine the point of time when the model test run can start [4]. During the test runs the air temperature is kept constant slightly above 0°C [5] until the last test run is executed and the pre-cooling procedure for production of the next ice sheet starts [6].

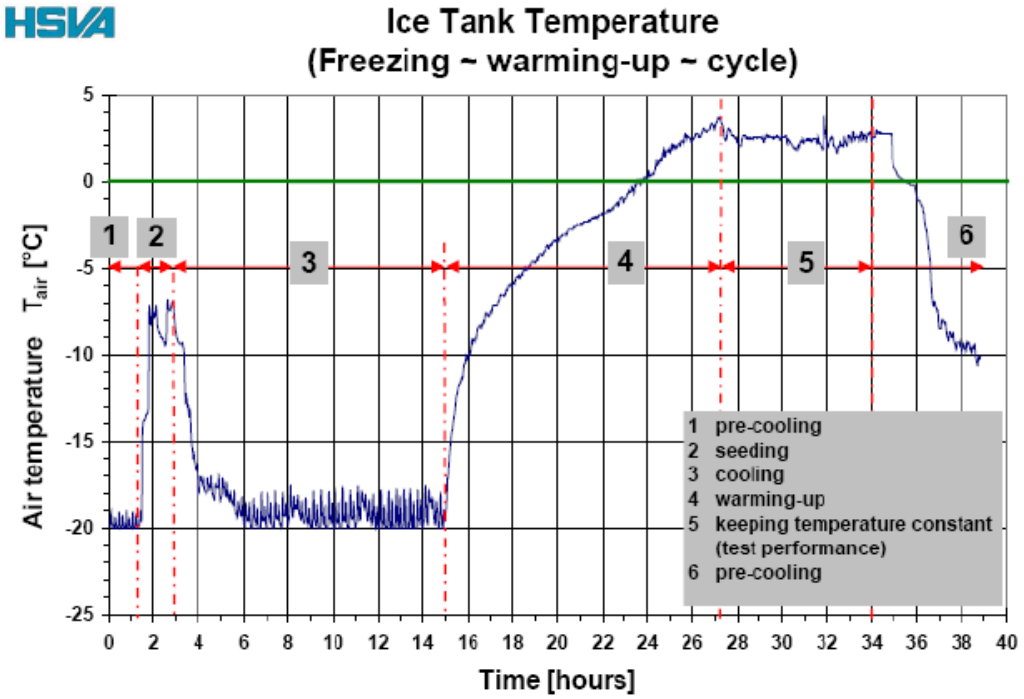

Figure 12. Example of the temporal temperature profile during a freeze-thaw-cycle.

ICE PROPERTIES

Since sea ice, in general, is an inhomogeneous, anisotropic, and nonlinear viscoelastic material, the mechanical properties of sea ice can be characterized as:

1) short-term, or generally brittle behavior, or
2) long-term, or generally ductile behavior.

The short-term properties usually considered are compressive, tensile, flexural, shear and adhesive strengths together with elastic modulus, Poisson's ratio and friction coefficient. These properties exist to a certain extent as a function of grain size, and crystallographic orientation, porosity and brine content, temperature, strain or stress rate, confinement and scale. The long-term properties are also a function of the same parameters but depend on time and the stress or strain rate that is usually held constant during testing (Sand, 2008).

Ice thickness

The thickness of sea ice is one of the most important ice parameters, because the way that ice fails is a function of the ice thickness. The ship performance of icebreaking vessels and ice forces on offshore structures exposed to ice depend on the ice thickness. Also the bearing capacity of ice sheets depends mainly on ice thickness, which has to be considered when trucks are moving or heavy loads are stored on the ice surface. Ice loads on offshore structures increase significantly with increasing ice thickness and the velocity at which vessels move through the ice is directly related to ice thickness (Timco and Weeks, 2010).

As a standard procedure in ice model testing at HSVA the ice thickness of a level ice sheet is measured at equal intervals along the center line of the basin prior to the test runs. These data

are used to draw an ice thickness profile of the undisturbed ice sheet. After the test run with a ship model or offshore structure model, ice thickness measurements are carried out at equal distances on both sides along the channel broken by the model.

Flexural ice strength

Although the flexural strength of ice is not a basic material property it is an important parameter which is used in ice engineering for design of icebreaking ships and offshore structures. Many real sea ice failures occur in flexure, e.g. pressure ice ridge formation, bending ice failure by icebreaking vessels and bending of ice on sloped and conical shaped offshore structures. Therefore the performance of flexural ice strength tests is justified.

The flexural ice strength is determined by creating a bending failure in the ice and measuring the failure load and the geometry of the specimen. It is most common to do this in-situ by cutting a cantilever beam and calculating the strength by means of the formulae derived from elastic beam theory $\sigma_f = 6\,PL/bh^2$, where σ_f is the flexural strength, P is the failure load, L, b and h are the length, breadth and thickness of the cantilever beam.

When using this equation it is assumed that the ice is isotropic and homogeneous, that the root of the beam is rigidly fixed and that there is no buoyant support of the beam by the water. However none of these assumptions is completely valid. Consequently the flexural ice strength is considered as a strength index.

Since the beam geometry can significantly influence the apparent strength (Timco, 1981; Tatinclaux and Hirayama, 1982) it is important to specify the beam dimensions. The relative size and geometry of the beam is also important since it is known for both sea ice (Frederking and Häusler, 1978) and freshwater ice (Svec and Frederking, 1981) that the apparent flexural strength depends upon the length to thickness ratio of the beam; the same is true for model ice.

It is important that a standard size and geometry is adopted in order to have a meaningful comparison of the flexural strength from one ice tank to another. If the beam is short in relation to its thickness, the failure mode involves shearing as well as bending. If the beam is very long in relation to its thickness, the buoyancy of the beam affects the apparent strength (Sutherland and Evers, 2013).

The IAHR Working Group on Standardizing Testing Methods in Ice recommends a beam length to thickness ratio of 7 to10 (Schwarz et al., 1981), however tests carried out by Timco indicate that, for model ice, the length to thickness ratio should be less than this in order that the strength is not a function of this ratio. Preliminary tests on the influence of the width to thickness ratio on the apparent flexural strength of the ice indicate that strength is not a strong function of this ratio (Timco, 1981). It seems that for tests on model ice, the length to thickness ratio of the cantilever beams should be of the order of 5 to7, and the width to thickness ratio should be 1 to 2.

To load the beams a screw-driven load cell can be used to determine the breaking load of the beam. The load cell gives information on the loading rate and time. A loading time of 1 to 2 seconds to failure is considered to be realistic to represent the time in which a model icebreaker would ride up and break the model ice. For most tests, the cantilever beams are pushed downwards. In the cases where ice fails against an inclined structure the strength should be determined by pull-up tests (Timco, 1981).

There are different approaches to determine the flexural ice strength as cantilever beam tests and simple beam tests. When doing in situ cantilever beam tests, the floating ice sheet is cut to form three sides of a beam. The fourth side is uncut and connected to the floating ice sheet (root of the cantilever beam). At the free end of the beam an increasing load is applied until the beam breaks. The test procedure is easy to conduct and the results are analyzed in terms of simple elastic beam theory (Timco and Weeks, 2010). Figure 13 shows the set-up of cantilever beam test.

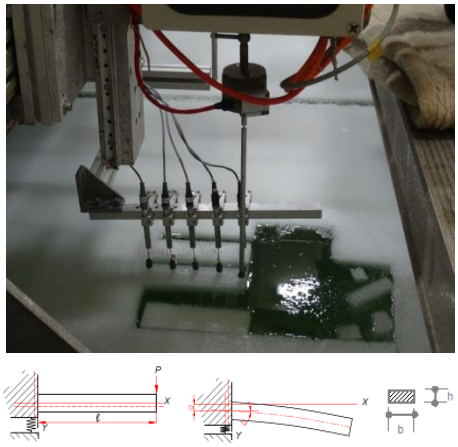

Figure 13. In situ cantilever beam test set-up with Linear Variable Differential Transformers (LVDT).

Effective modulus (elastic strain modulus)

The determination of the elastic strain modulus is based on the measurement of load and deflection of either a beam or a plate. Taking the geometry involved the strain modulus can be calculated by means of equations which are derived from theory. It is important to specify the technique used for the measurements, because various measurement techniques result in different *E* values in the same ice. Currently the "plate technique" as proposed by Sodhi et al. (1982) and the beam methods as proposed by Tatinclaux and Hirayama (1982) are used in ice tanks. The latter one may lead to a better method for comparing the model and full scale modulus, because more information and comparisons have been made both in laboratories and field tests.
Similar to the ice strength, the elastic strain modulus E is scaled by the geometric scaling factor of the tests. Since the proper scaling of this parameter in model tests is important, an acceptable test must be defined to measure this property. Basically, it can be measured using either static or dynamic techniques (Timco, 1981).

In the static method, the strain modulus can be determined using either a beam or plate approach. In the former, the modulus is determined by measuring both the load and deflection characteristics of a cantilever beam during loading to failure, whereas in the latter the modulus is determined by monitoring the deflection of the ice sheet as it is loaded with a known increasing load. In ice tanks which measure the strain modulus, the latter technique is usually preferred since it integrates over a large area of the ice sheet and is both simpler and quicker to perform.

In the flexural strength test, the ice can be loaded with either with a screw-driven apparatus in series with a load cell (Figure 14a) or dead weights in discrete increments (Figure 14b), or. During loading, the deflection can be measured either adjacent to or slightly away from the

load (within one characteristic length) by either dial indicator gauge, LVDT or LASER-sensor which gives a continuous recording. On the other hand, the dead weights and dial indicator are much simpler and faster to use and may serve as a method of quickly determining the modulus prior to a model test.

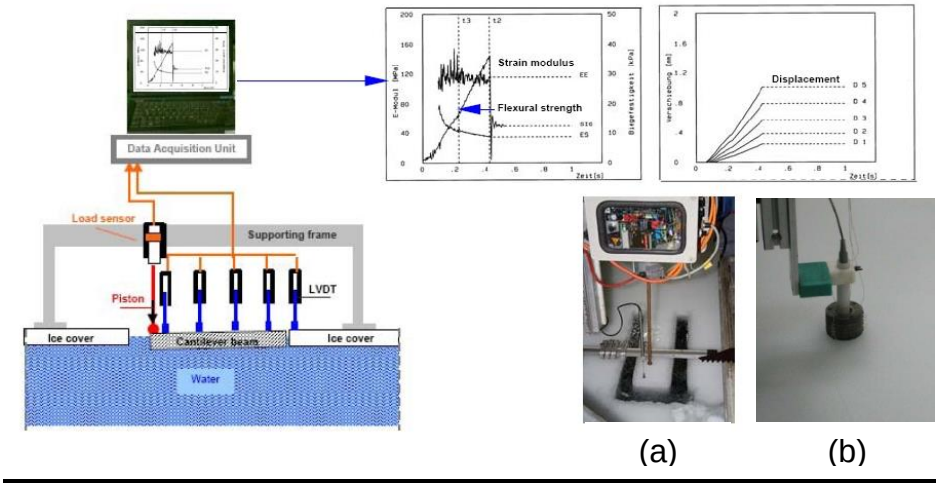

Figure 14. Determination of elastic strain modulus: cantilever beam with LVDTs (a) and plate method (b).

Uniaxial compressive strength

Measurement of the compressive strength of model ice is important, especially for the horizontal loading direction, when ice impacts rigid vertical structures it often fails in a crushing mode.

After the ice sample has been collected from the field or grown under laboratory conditions, rough cutting of prismatic ice blocks or cylindrical cores is advisable in order to obtain manageable sample size. Cubes have also been used conventionally, but the results are unreliable hence not recommended for uni-axial compression strength tests.

In the conventional uni-axial compression test, axial force is applied to the ends of a prismatic sample or circular cylinder through compliant platen that make direct contact with the test specimen. Friction between platen and specimen produces radial restraint, so that there is a triaxial state of stress near the end planes; the triaxial field is significant over an axial distance from the end planes of about one specimen radius. Placing a highly compliant sheet (elastic or plastic) between platen and specimen often changes the sign of radial end forces, but does not eliminate the triaxial stress state. The usual procedure for testing ice in uni-axial compression is to accept positive frictional restraint at the specimen end planes and to use a specimen that is long enough to provide a mid-section that is reasonably free from end-effect stress perturbations (length/diameter ratio of 2 to 3) (Schwarz et al. 1981).

At HSVA uni-axial compression tests are carried out on a rigid closed loop controlled testing machine by a hydraulic piston for load application. The specimen for compression tests should be sampled from the same location in the ice tank, where in situ flexural strength tests are being carried out at the same time and the ratio between flexural strength and compressive strength of the model ice can be determined.

Prismatic ice samples having a size of *1h x 2h x 4h*, with *h*= ice thickness, are cut and placed in between the two loading plates of the test frame. Compliant platens or thin sheet of compressible material is used in order to avoid sliding of the specimen and to apply uniform axial load to the specimen. The applied load and crosshead movement are recorded and the results can be presented as load deflection curves. Figure 15 shows the testing machine and the hydraulic aggregate in the refrigerated laboratory.

Figure 15. Uni-axial compressive strength test: (a) test set-up (b) prismatic ice sample placed between load platens (c) failure of ice sample during compressive failure.

Crushing strength (indenter tests)

One practical method is the indenter test. The indentation test is done in a place where the indenter can be put into the ice sheet through an existing hole (holes for beam or density tests). The device is placed vertically as shown in Figure 16. The tests are typically performed at several speeds, such as 30, 10, 3, and 1 mm/s.

The compressive strength is calculated using equation (1):

$$\sigma_c = \frac{F}{ci * mkbh} \tag{1}$$

where

F = force (measured)
m = shape factor (round structure 0.9)
k = contact factor (0.4 - 0.7)
h = ice thickness
b = diameter of indenter
ci = constant, function of *b/h*

Figure 16. Indenter test with large indenter (diameter 250 mm) outfitted with tactile sensors to measure local ice pressure distribution along the perimeter (a) and small indenter (diameter 60 mm (right).

Ice density

The determination of the density of model ice using the standard technique - cutting a sample block, measuring its dimensions (i.e. volume) and weighing it - has several inaccuracies, the primary one being that a large number of the liquid impurity pockets in the ice drain out when it is removed from model ice sheet. Nevertheless, the technique can be used to obtain semi-quantitative density values, although measurements of the freeboard of model ice may prove to be a better method of ice density determination (Timco, 1981).

A more advanced method is the density measurement by the principle of displacement. Ice samples of 120 mm times 120 mm size are cut from the existing ice sheet at locations where cantilever beam tests are carried out and stored in a plastic bowl filled with water from the ice tank in order to avoid any drainage.

The specimen is submerged and the displaced water volume is collected and weighed. The buoyancy force is measured by means of a load sensor. The test set-up for the density measurement is illustrated in Figure 17.

Figure 17. Set-up for determination of ice density

The ice density is calculated by equation (2):

$$\rho_i = \rho_w - [\, F_b / (V_d * g) \,] \quad (2)$$

where

ρ_i = ice density [kgm^{-3}]
ρ_w = water density [kgm^{-3}]]
F_b = buoyancy force [N]
V_d = displaced water volume [m^3]
g = acceleration due to gravity is 9.814 [ms^{-2}]

Friction coefficient

A testing apparatus developed and designed at HSVA is used to determine the dynamic ice friction coefficient. During the varnishing process of the model a plate of same material as the model is painted at the same time to ensure same surface characteristics. The plate is fixed on the carriage of the friction apparatus (Figure 18a) which can be moved back and forth. The ice specimen is adopted in a frame (Figure 18b), where two slightly pre-stressed load cells are mounted between this frame and the support and remains stationary while the carriage moves back and forth. A schematic diagram of the friction device used at HSVA is illustrated in Figure 18.

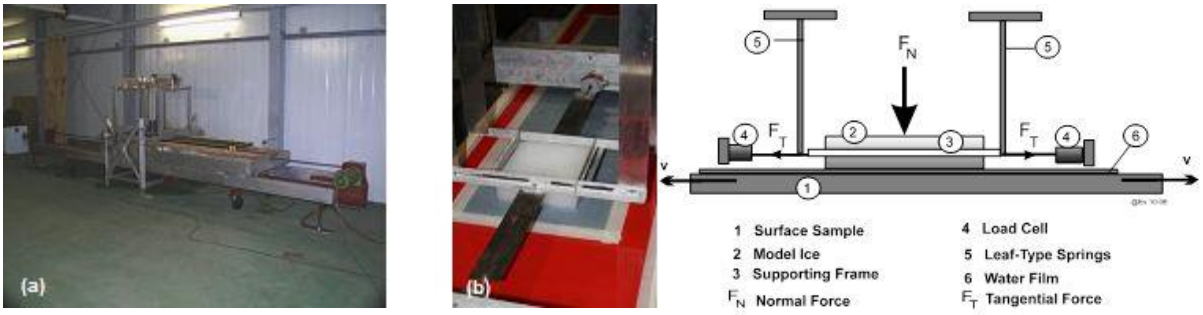

Figure 18. Ice friction testing device (a) and ice specimen adopted in a frame (b) and schematic diagram (right).

The tangential force is measured by two load cells. Two different normal loads, e.g. 50 and 100 N, are applied by adding ballast weights to the weight of the ice specimen. For each normal load 10 test runs are carried out. An average value is calculated giving the dynamic friction coefficient between the ice and the tested (hull) surface of the model.
The dynamic friction coefficient is calculated according to Coulomb's friction law:

$$C_{if} = F_t / F_n \quad (3)$$

where

C_{if} is the dynamic friction coefficient
F_t is the mean value of measured tangential force in [N]
and F_n is the normal load in [N]

The ice friction coefficient is inversely proportional to the normal load applied to a specimen, i.e. the higher the normal load, the less the ice friction coefficient C_{if}. Typical values are $0.04 < C_{if} < 0.14$.

It is recommended to carry out friction tests at least once during a testing campaign. The friction coefficient should be determined for the case that the top surface of ice specimen is in contact with the plate with the same surface property of the model. The tests should be conducted under dry and wet conditions.

MODELLING OF VARIOUS ICE CONDITIONS

Level ice

Level ice is a homogeneous ice sheet unaffected by any deformation with consistent ice thickness. The production is described exemplarily for HSVA's current model ice. It is frozen from a 0.7% sodium chloride solution in the natural way, i.e., the ice surface is exposed to cooled air. The preparation of the ice sheet is started by a seeding procedure.

Main parameters to be measured in level ice sheets are:

- flexural strength (when bending failure occurs predominantly)
- uniaxial unconfined compressive strength (when crushing failure occurs predominantly)
- ice thickness along the broken channel
- width of broken channel
- ice density
- modulus of elasticity (optional)

Figure 19 shows as an example the ice-vaning scenario of a moored Floating Production Unit model (FPU) in level ice.

Figure 19. Ice-vaning test with a moored FPU in level ice.

Broken ice floes

For ship navigation in broken ice (ice floes) conditions it is essential to consider the floe size and the ice coverage or ice concentration. Usually the two terms “ice coverage” and “ice concentration” are used to describe the ratio of ice floes and the area of open water referenced to a unit area (e.g. 1 km^2), thus both terms have the same denotation. The unit of ice coverage or ice concentration is given as tenth or in percentage. As an example six-tenths or 60% coverage means that 60% of a unit area (100%) is covered with ice.

Also for ice management around fixed or floating structures broken ice conditions have to be taken into account. Thus the performance of tests in broken ice is in many cases part of the model test program.

When modeling broken ice conditions a predefined parental level ice sheet has to be prepared first and then cut in pieces corresponding to the required size and shape, which is illustrated in Figure 20.

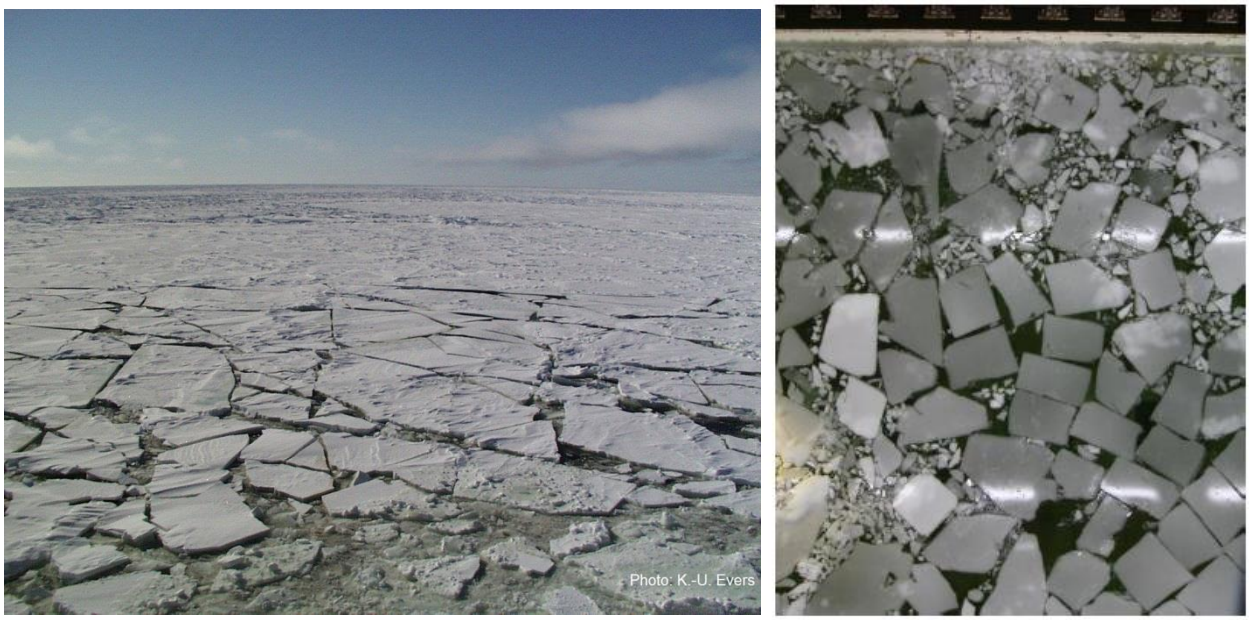

Figure 20. Ice floes in full scale (left) and ice floes in model scale produced in the ice tank (right).

The preparation of ice floes in the ice tank is done manually by cutting the parental level ice sheet in pieces of required size and shape according to model scale factor and distributing them to achieve the required different ice concentration (e.g. 60% to 90%). Figure 21 shows the preparation of ice floes with different sizes and the ice floe arrangement at the end of the ice tank (about 90% ice concentration).

The shape of ice floes could be quadratic-, rectangular- or rhombus shaped. Circular shape floes seldom occur except when pancake ice is taken into account. It should be noted that the most realistic movement of ice floes in the tank can be achieved by rhombus shaped floes, while quadratic shaped floes mostly do not rotate when the vessel encounters an ice floe field.

When the model encounters quadratic shaped ice floes they are pushed together and usually do not rotate, when the ice concentration is high. At high ice concentrations, e.g. c = 90% and more, the sidewalls of the basin may affect the flow of ice floes (ice clearing around the model) due to the confinement.

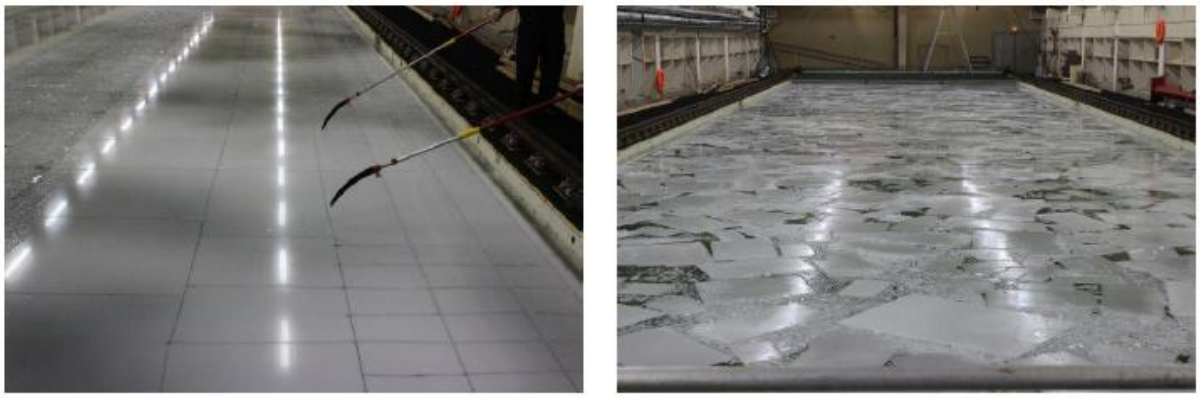

Figure 21. Production of ice floes in the ice tank (left photo) and 90% ice concentration (right photo).

Parameters to be measured:

- ice thickness
- ice coverage respectively ice concentration (before test run starts)
- ice floe size

Method to determine parameters:

- calliper gauge (ice thickness)
- documentation by photography (ice concentration, ice floe size and shape)

The ice concentration can be determined by means of photogrammetry techniques and image processing software. The processing of images is done with the main focus on the static ice concentration in advance of the model tests over the total ice tank length.

Before each test in broken ice, several pictures are taken by a digital still camera from a certain level above water surface along the ice tank. If the camera lens does not capture the entire tank width, two pictures or more, depending on the width of the ice tank, have to be taken along the width.

By image processing all of those pictures are stitched together using the overlap that is among them. The resulting images are evaluated to obtain the ice concentration. The results of ice concentration are based on a technique using a pixel analysis. To evaluate the image pixel by pixel it has first to be converted to grey scale. Then each pixel has a value between 0 (pure black) and 255 (pure white). A set threshold value divides the pixels into two groups; grey scale values below the threshold become black and those above become white. In this way a black and white (or binary) image is created. An example is given in Figure 22. With the ratio between the black and white pixels the coverage of ice on the water surface can be determined. The results of the pixel analysis from the overall pictures from top of the ice tank are given as global ice concentrations. A more detailed description of the method is given by van der Werff (2012), van der Werff et al. (2012), Haase et al. (2012), Zhang et al. (2012) and Sutherland and Evers (2013). Image editing software ImageJ ™ is used to analyse the images and gives information about the amount of ice floes, average ice floe size [L^2] and ice concentration [%].

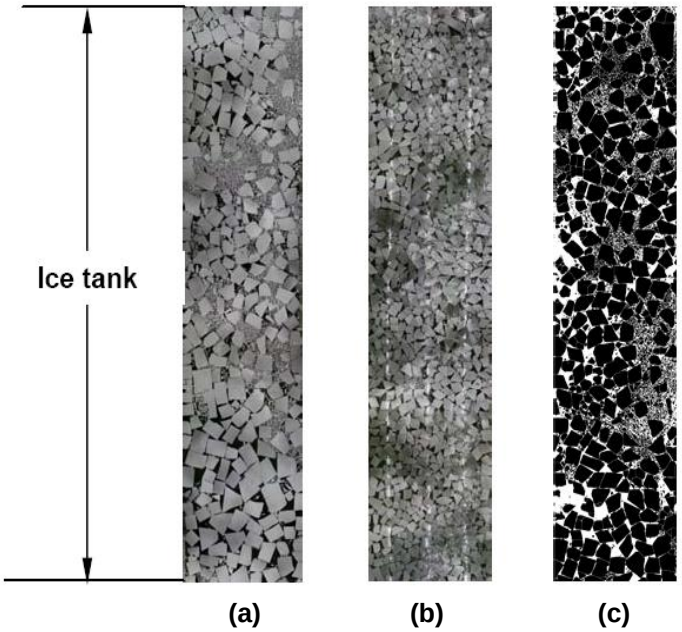

Figure 22. Examples of stitched pictures (a-b), (c) example of binary image. The pictures show the ice coverage of the entire ice tank area.

Figure 23 shows examples of a moored conical drilling unit and a ship model during dynamic positioning in broken ice conditions the ice tank.

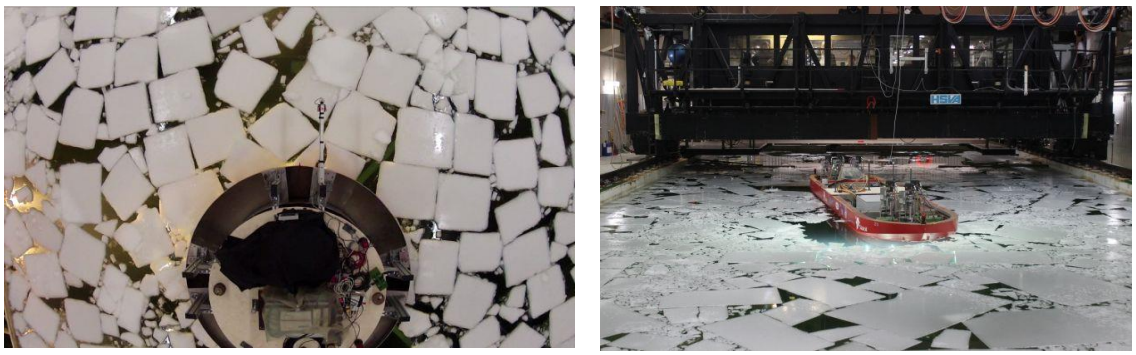

Figure 23. Model of a moored conical drilling platform (left) and ship model (right) in broken ice conditions.

Brash ice

According to the *World Meteorological Organisation* (WMO) the term “brash ice” is defined as accumulations of floating ice made up of fragments not more than two meters across. Brash ice forms quickly during frequent passages in an ice channel filling the channel with ice fragments behind the vessel. As the broken ice consolidates between each passage, new brash ice is successively produced resulting in increased brash ice thickness which leads to higher vessel resistance.

Model tests in brash ice are required to demonstrate that a ship has sufficient propulsion power to navigate safely along a route in the ice. This is necessary for issuance of the

appropriate ice class of the ship. Figure 24 presents a typical brash ice channel from the northern Baltic.

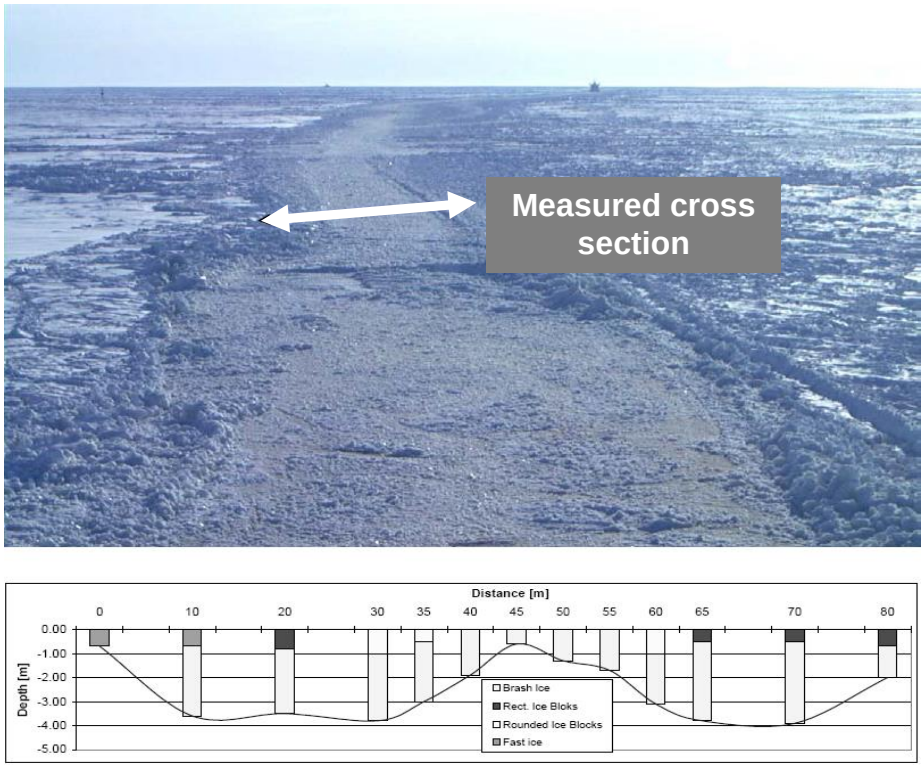

Figure 24. A photograph of a brash ice channel leading to the Finnish port Kemi and the measured cross section of the channel (after Riska, 2014).

Preparation of brash ice channels in model ice sheets

At HSVA a parental level ice sheet of adequate thickness is produced according to the standard preparation procedure. After a predefined level ice thickness has been achieved, the air temperature in the ice tank is raised. When the air temperature is close to -3°C, an ice channel with straight edges is cut into the ice sheet. This is done by means of two ice knifes being pushed by an auxiliary carriage. Thereafter, the ice stripe between the two cuts is manually broken up into relatively small ice fragments using special ice chisels (Figure 25).

In order to obtain a brash ice channel with desired brash ice thickness according to the Ice Class guidelines, the ice fragments in the channel have to be compacted. The compacting process is done in sections by means of a channel-wide grid, starting from the rear end of the channel.

For a second test run with larger brash ice thickness the ice fragments will be rearranged in the channel and furthermore compacted. Since the channel filled with brash ice becomes shorter due to the compacting procedure, some of the level ice from beside the forward part of the channel is additionally broken up and refilled into the remaining part ice-free section of the channel.

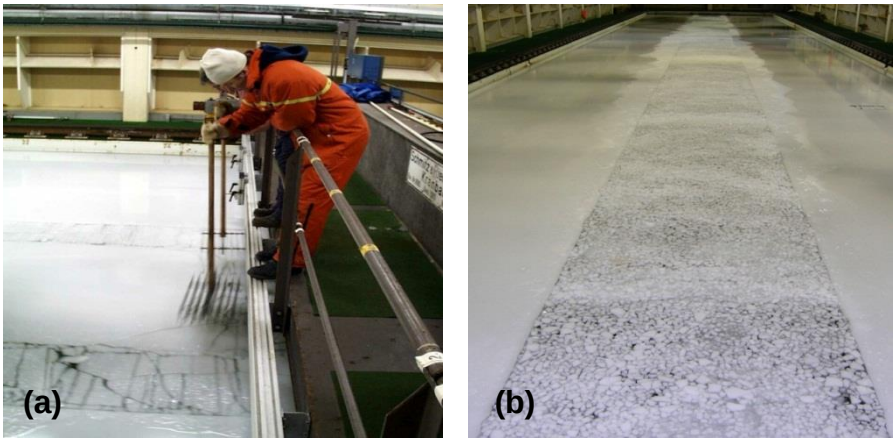

Figure 25. Preparation of brash ice fragments from level ice by means of special ice chisels (a) and channel filled with brash ice fragments (b).

Typically, the brash ice thickness is measured before the test run starts at 7 locations across and in 1m distances over the whole length of the brash ice channel. A special device is used for the measurements. This device consists of a slide gauge with a perforated plate mounted under a right angle at the lower end of the gauge. With the slide gauge the thickness of the brash ice is measured whereby the ice is floating in the water. This is done by slightly pulling the lower plate up against the bottom of the brash ice fragments. The top plate is lowered in such way that it just get in contact with the top of the brash ice. The porosity of the brash ice is calculated based on the total area and the thickness of the level ice being used to generate the brash ice. Figure 26 shows an example of a model in a brash ice channel.

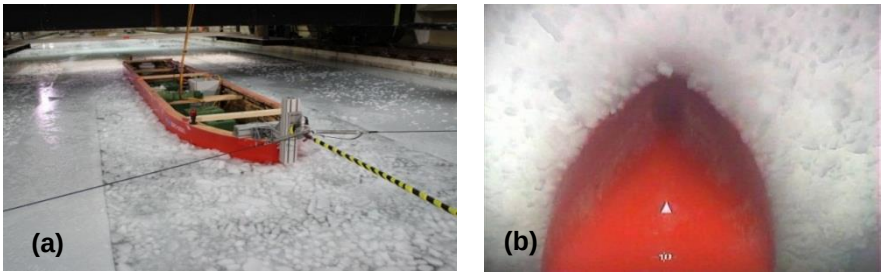

Figure 26. Model test in a brash ice channel (a) and view from underwater towards the bow of the vessel in brash ice channel (b).

Pressure ice ridges

The formation of pressure ice ridges in an ice cover is a result of changing stress regime within the plane of the ice sheet. The ridges originate from the interaction between ice floes as they collide with each other cause by wind and/or current driving forces. Pressure ridges consist of angular ice blocks of different sizes which pile up on the floes (sail) or submerge below the floes (keel). Pressure ice ridges which are grounded as a result from interaction between fast ice and drifting pack ice are called Stamukhi or grounded hummocks, according to *WMO Sea Ice Nomenclature*.

The main geometrical characteristics of pressure ice ridges are keel depth, sail height and thickness of consolidated layer as illustrated in the schematic diagram (Figure 27). In addition the parameters ice block size, porosity and bulk density characterize the ice ridge.

During the summer the ridge can undergo a substantial amount of weathering. During the weathering process the salt drains out of the ice blocks (brine drainage). When a ridge undergoes freezing a consolidated layer is formed, i.e. at cold air temperatures the water between the individual ice blocks is frozen. As a result the porosity is reduced and the bulk density increases. This has an impact on the mechanical properties and is associated with an increase in ice strength. The keel depth of a ridge is much larger than its sail height and can reach up to more than 40 m. Typically the the keel depth is about 4 - 5 times the sail height and the keel width is also 2 - 3 times wider than the sail.

Figure 28 shows an area of first year ridges in the Kara Sea investigated during an Arctic expedition in 1998. From offshore engineering and ice navigation perspective, pressure ice ridges are of particular interest and subject of investigation.

Firstly, drifting ice with embedded ridges, in particular when they are consolidated, causes high loads on offshore structures.

Secondly, when pressure ice ridges drift into shallow water areas, the ridge keel may contact the seabed and represents a risk of scouring for pipelines installed on the sea bottom.

Thirdly, when taking into account that ridged ice makes up to 40% of the overall mass of artic sea ice, ice ridges have a significant impact on ship navigation in cold regions, because these ice features may impede the navigation in ice.

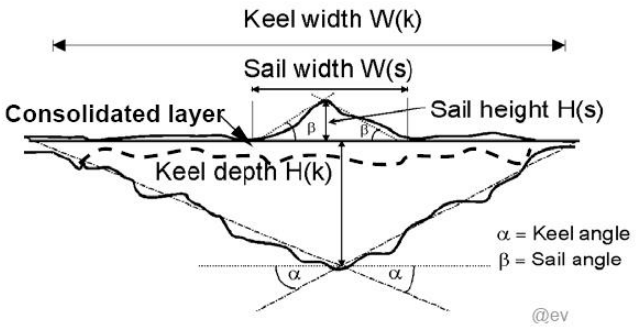

Figure 27. Main characteristic ridge dimensions.

Figure 28. First year pressure ice ridges in the Kara Sea, photo was taken during the ARCDEV expedition 1998.

Ridge production techniques

There are various methods for the production of model pressure ice ridges, which are used depending on the available test devices in the various ice tanks. The method described below is used at HSVA.

Prior to the ridge building process ice and air temperature as well as ice thickness in level ice are measured along the mid-line of the tank. When a specific ice temperature, which might be different in the various ice tanks, is achieved the ridge building process starts. The thickness and strength of the consolidated layer in the ridge strongly depends on the temperature and strength of the initial ice sheet used to build the ridge. The ice temperature is measured in the level ice sheet 2 cm below the ice surface, while the air-temperature is measured 2 cm and 1 m above the ice surface.

Depending on the required ridge geometry parameters (e.g. length, width, sail height and keel depth) the required volume of ridge fragments taking into account the ridge porosity is calculated. If the volume and porosity is known the length for cutting the ice sheet into stripes is calculated.

The width of the stripes is adjustable depending on the required size of ridge fragments. Thereafter the ice is cut along the sidewalls, and a cut transverse to the longitudinal axis of the tank is made at the spot where the ridge is to be built. At this spot a box girder with inclined face is put across the tank supporting the ridging process (Figure 29).

The free floating ice sheet with stripes is pushed against the ridge bar by means of the towing carriage's pushing board. During the ridge formation the ridge beam is successively stepwise moved forward (step 1, 2,…4 in Figure 30). The length and thickness of the floating ice sheet, and the bulk density determine the volume of an ice ridge. By this way a ridge of defined ice mass can be generated. The size of the ridge is controlled by the number of dislocations of the ridge beam. Smaller dislocations lead to a narrow ridge with larger keel depth. Wider ridges with smaller keel depth can be produced when the ridge beam is dislocated several times.

The ridge has a typical natural underwater profile (triangular or trapezoidal) and is embedded in level ice. If desired the upper layer of the ridge can be consolidated. Figure 30 shows the schematic principle of ridge preparation procedure.

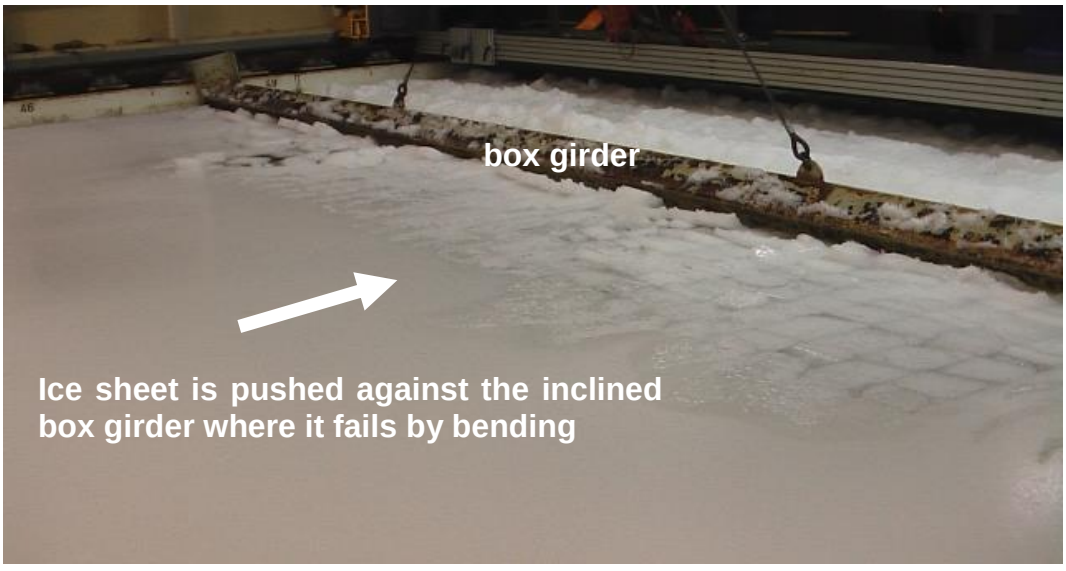

Figure 29. Principal ridge preparation procedure.

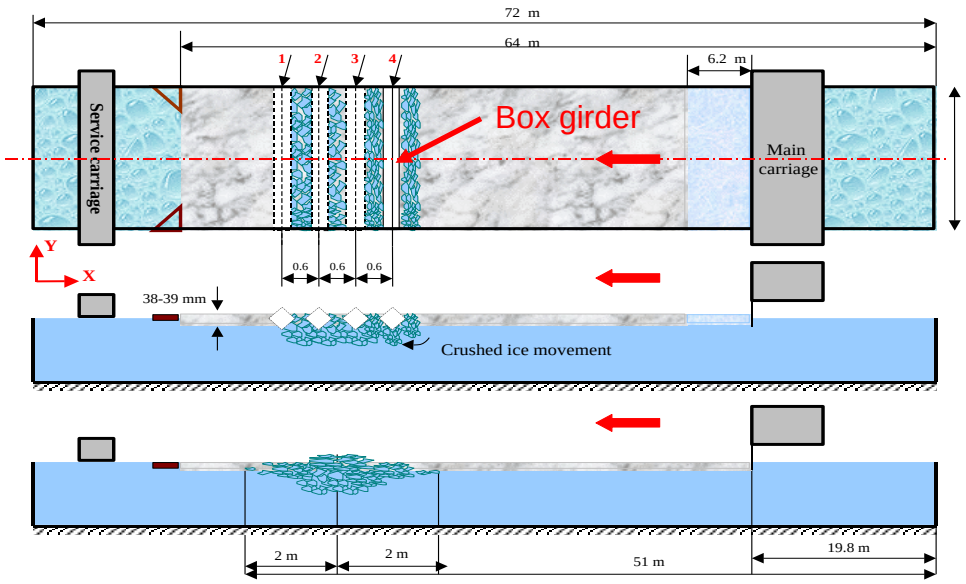

Figure 30. Schematic diagram of model ridge preparation procedure at HSVA (example).

The number of ridges to be built in one ice sheet depends on the dimension of ridges and the length of the ice tank. It is recommended that the distance between two ridges should be larger than 2.5 times the ship length to ensure that the vessel can pass the ridge completely before penetrating the second one. Figure 31 shows a model ice ridge embedded in a level ice sheet after it was built (a) and ad-frozen ridge fragments from the consolidated part of the ridge (b-c).

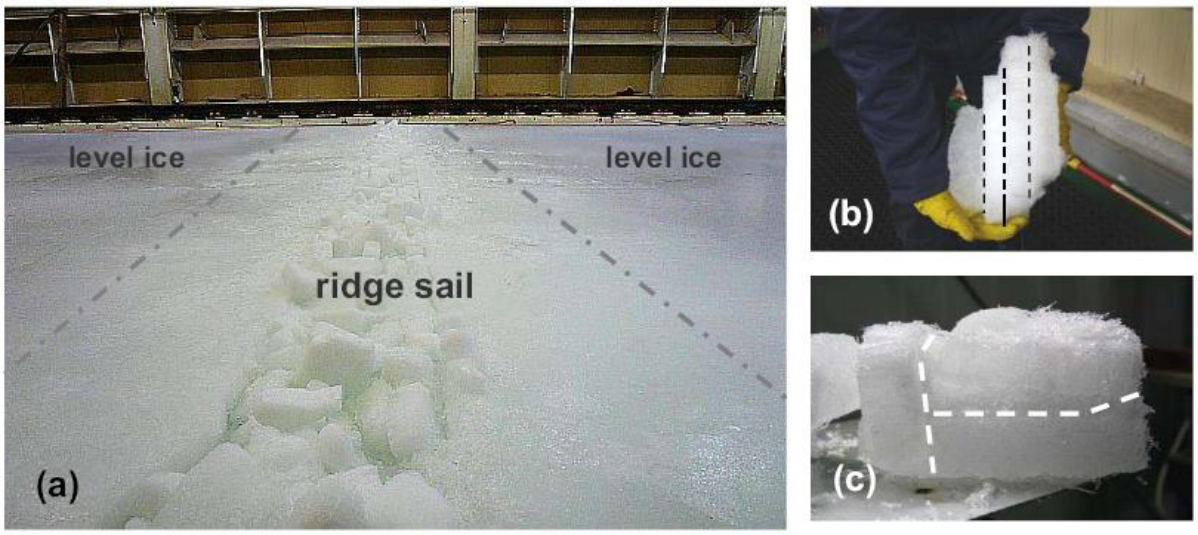

Figure 31. Ice ridge embedded in level ice (a) and ad-frozen ridge fragments from the consolidated layer (b-c).

After a ridge has been built the keel depth and sail height are determined by profiling. In general three profiles are taken preferably in the area of the model trace (portside – center –

starboard). This is done by pressing a stick in equidistant intervals through the ridge. At the lower end of the stick a cross-bar (Figure 32) is activated and the stick can be lifted upwards until a certain resistance indicates the bottom of the ridge. The keel depth is indicated at the reading line (yellow circle) by a marker in the upper part of the stick (Figure 32). From the measured data a profile of the ridge sail and keel can be plotted (Figure 33).

Alternatively the underwater contours of the ridge can be profiled with acoustic echo sounder and the sail topography above water by laser level (Sutherland and Evers, 2013).

Ice rubble fields are produced according to the same procedure as ice ridges are built as described above. An example of an unconsolidated rubble ice field in the ice tank is shown in Figure 34.

Figure 32. Ridge profiling device to determine keel depth and sail height.

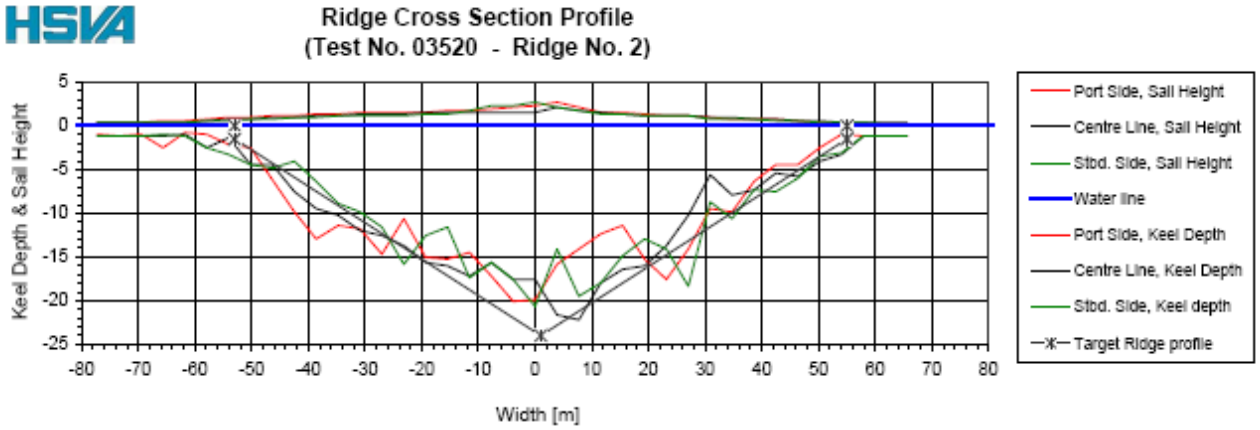

Figure 33. Model ridge cross-section (data are given as full scale values in meters).

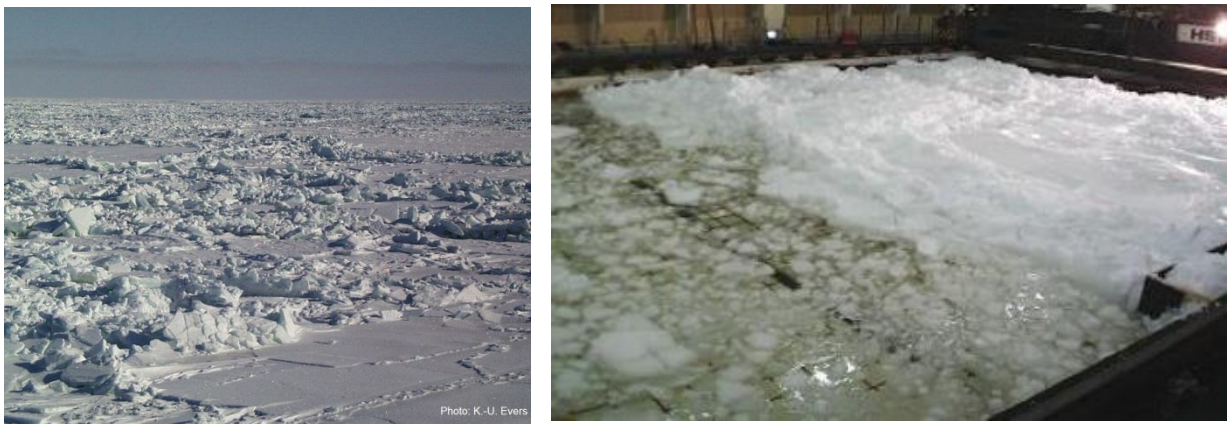

Figure 34. Ice rubble field in the Kara Sea (left) and ruble field modeled in the ice tank.

SELECTED PROJECTS

Project: Model testing of moored structures in ice

Numerous ice model test projects with fixed and moored floating structures (e.g. (i.e. FPU, FPSO, shallow draft buoy and Spar-platform, etc.) to support the design with respect to the operability in various ice conditions (i.e. level ice, pressure ice ridges, ice floes, ice rubble fields and managed ice) have been carried out at HSVA.

The choice of a proper scale plays an important role, because the environmental conditions (ice , water depth, current, etc.), dimensions of the structure/vessel, the dimensions of the ice tank, and the configuration of the mooring system are to be considered. For the model test campaign, in general, the full scale situation has to be modelled as accurate as possible, Deviations of modelled test set-up from full scale set-up cannot always eliminated, because some features have to be simplified and need adaption to the available infrastructure.

The dynamic behaviour of the moored vessel and its interaction with the mooring system is of great importance and has to be simulated as accurate as possible in the model tests. For the conceptual design of the vessel and the mooring system the ice forces, restoring forces, mooring line forces, vessel displacement, vessel motions (heave, pitch, roll and yaw) have to be determined. Also the interaction between submerged broken ice floes and the turret respectively mooring lines is of interest (Evers and Jochmann, 2011).

The first moored floating structure in ice was tested at HSVA about 35 years ago. HSVA was contracted by Gulf Canada Ltd. to develop the design of the hull shape of the well-known conical drilling unit “Kulluk” in order to deflect submerged broken ice. Subsequently comprehensive ice model tests were conducted in level ice and ridges. Within the following years other concepts (Figure 35) like Arctic shuttle tanker, STL, SPM, offloading buoys, shallow draft buoys, moored FPU and FPSO were subject of ice model tests at HSVA (Evers and Jochmann, 2011).

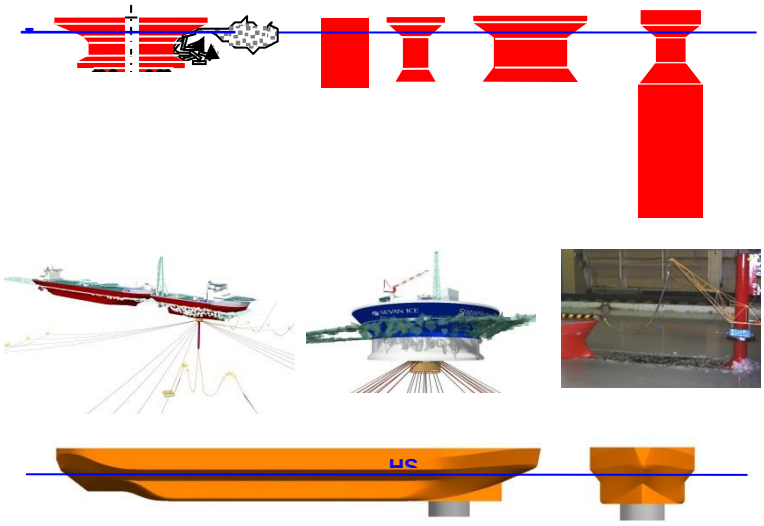

Figure 35. Different concepts of moored floating structures and vessels tested in ice at HSVA

In general the moored floating structure should be capable to break level ice sheets associated with ridges and ice rubble fields and should also be able to disconnect from the mooring system in the case of iceberg collision risk. A reconnection at a later date should be possible.

Ice management by means of purpose built ice breaking supply and standby vessels may be necessary to ensure maximum operability in case of extreme ice conditions.

The hull at the waterline should be designed to allow the level ice and the consolidated layer of the ridge to fail by bending. Even more important is the hull design with respect to ice clearing, i.e. the transportation of broken ice floes and ridge fragments around the floating structures respectively vessels. In particular for buoys the hull diameter below the waterline should be reduced as much as possible to avoid serious accumulation of broken ice pieces around the structure, which consequently increases the effective diameter and generates higher ice loads.

Set-up of a moored Arctic Tandem Offloading Terminal (ATOT)

The Arctic Tandem Offloading Terminal (ATOT) is a concept for offshore offloading in ice-covered waters . The concept exists of two units: a turret moored Offloading Icebreaker (OIB) and a shuttle tanker moored in tandem at the OIB aft as shown in Figure 36a-b (Bonnemaire, et al., 2008).

The OIB design basis is that it should be able to withstand the interaction from severe ice conditions, such as unmanaged deep ice ridges in straight drift. The operational strategy is that the tanker may disconnect and reconnect to the OIB if required, however the OIB should be able to remain moored at the location as long as possible. The OIB prototype is thus moored on mooring lines fixed on a sub-surface loading buoy connected inside a turret. The OIB is optimised for icebreaking with an icebreaking spoon bow and reamers on the side to increase the manoeuvrability in ice and break a wider channel to reduce the ice forces on the tanker. (Bonnemaire, et al., 2010)

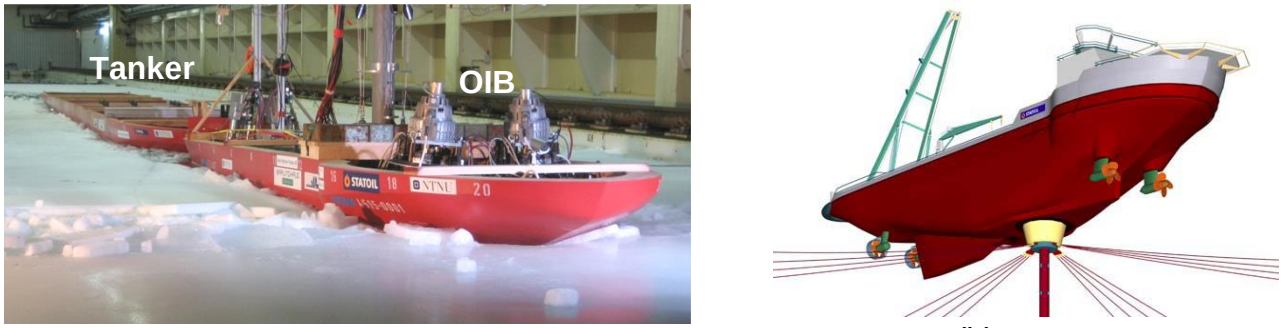

(a) (b)

Figure 36. The OIB with 4 pods penetrating a ridge, with the tanker moored in close tow in the background (model scale 1:24) (a) and artist impression of OIB (b).

For the tests a "dry" mooring system as shown in Figure 38 and Figure 39 was designed and connected to the transverse carriage at the rear of main towing carriage facilitating the execution of manoeuvring or dynamic positioning tests in the ice tank with free sailing icebreaking vessels in level ice, ridges and ice rubble fields.

This device is very suitable for the execution of tests regarding slow or rapid ice drift change scenarios. In this case the turning radius of the vessel and the ice drift speed can be varied, when the model is guided through the ice by the towing carriages and the ice sheet is kept stationary (Figure 37).

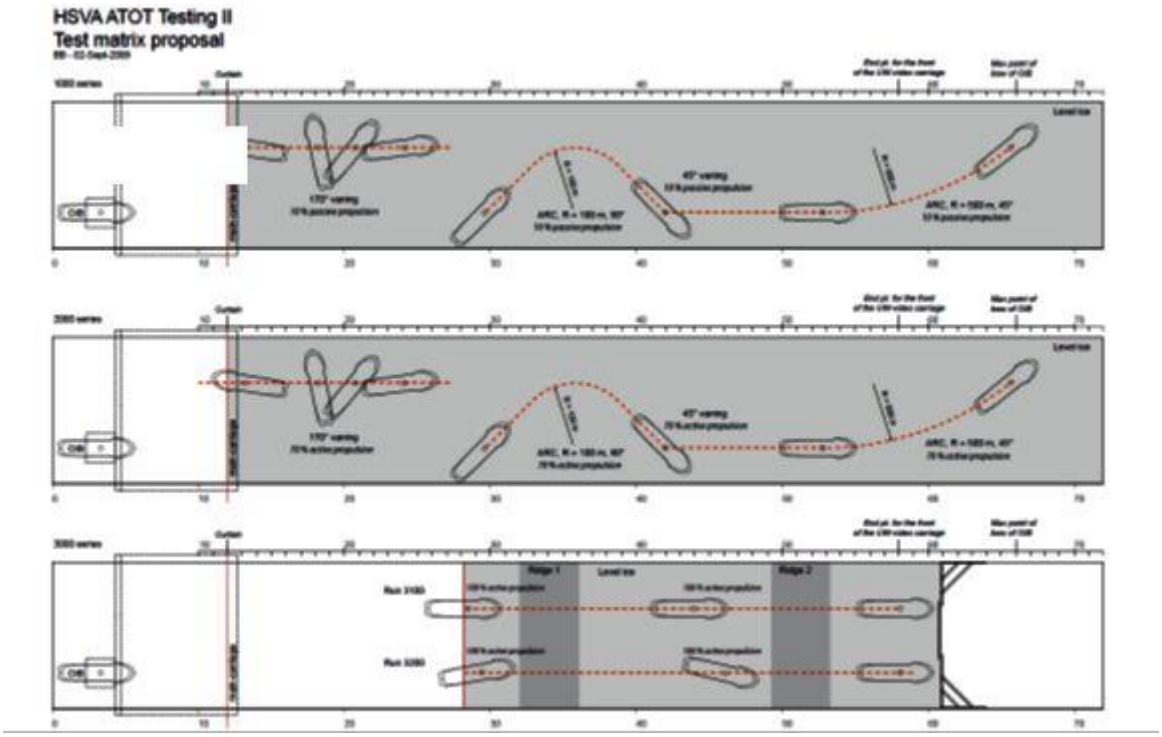

Figure 37. Schematic diagram of slow or rapid ice drift change scenarios, the turning radius of the vessel and the ice drift speed is varied.

For practical reasons, a "dry" mooring system mounted "upside down" above the model is more convenient to handle, i.e. easy access to the mooring system without discharge of tank water (Figure 38). In the test campaign the model was tested in different ice conditions (e.g. level ice, ridges, ice rubble and managed ice).

Figure 38. OIB model with "dry" mooring system (a); FPU model in fixed mode connected to the transverse carriage (b).

Figure 39 presents a schematic diagram of the dry mooring device. A vertical column is fixed to the bottom of the vessel by means of a universal joint and a triaxial load cell. The column is thus fixed in surge, sway and heave to the vessel. However the column is free to heave in the mooring frame. The column is mounted on the transverse carriage which can move simultaneously with the main carriage in x and y-directions. On each beam a coil spring - mooring line and load cell system is mounted, that controls the force in surge and sway between the vessel and the towing carriage.

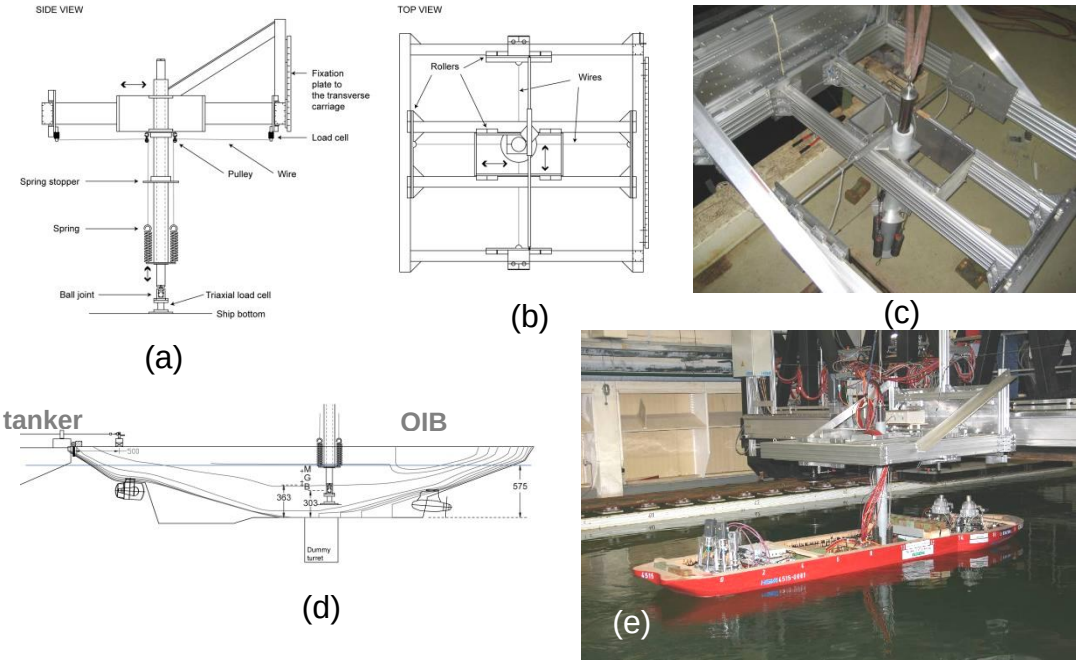

Figure 39. Schematic diagram of the dry mooring device (Evers and Jochmann, 2011).

Project: Investigation of influence of structural compliance and slope angle on ice loads and dynamic response of cylindrical and conical structures

Slender cylindrical structures are often found in offshore applications such as wind turbines, legs of GBS etc. Their simple, cost-efficient shape provides reasonable open water properties. However, ice loads on vertical structures are generally high, and flexible cylindrical structures may be set into lock-in vibrations due to structural feedback to the ice load. Such vibrations should be avoided to minimize the risk of severe structural damage (Ziemer, et al., 2015)

Model tests in ice have been conducted with cylindrical and conical, compliant structures exposed to drifting level ice to investigate the influence of slope and compliance on the ice load and its breaking frequency. Main goal of the test campaign was to study the importance of structural feedback during ice-cone interaction. Four shapes were tested: 50°, 60°, 80° and 90° slope angle. The cylinder was tested in order to define the worst case scenario regarding magnitude of ice load and severity of ice-induced vibrations. Stiffness and natural frequency of the structure were chosen similar to typical values for offshore wind turbine support structures. All shapes were tested both in a compliant and fixed configuration.

The breaking frequency was found to be more pronounced for the lower slope angles where the ice failed in flexural failure only, while a transition to crushing failure as observed on a cylindrical structure takes place at 80° cone angle already. This results in significantly higher ice loads on the 80° cone than on those with lower angles, but a reduced risk of severe ice-structure interaction due to the unsteady nature of the mixed mode breaking process. Although the breaking frequency is rather constant e.g. during ice impact on the 60° cone, it was not possible during the model tests to match the ice drift speed and the dynamics of the structure in a way that causes resonance. However, model test results prove that there is a risk of conical structures with low natural frequencies and low stiffness in ice plane being excited by periodic ice failure in their natural frequency, thus response amplification may take place and pose a risk to the structural integrity of conical offshore structures exposed to sea ice (Ziemer, et al., 2015).

Figure 40 shows a schematic diagram of the test set-up and upward bending ice failure on a conical structure.

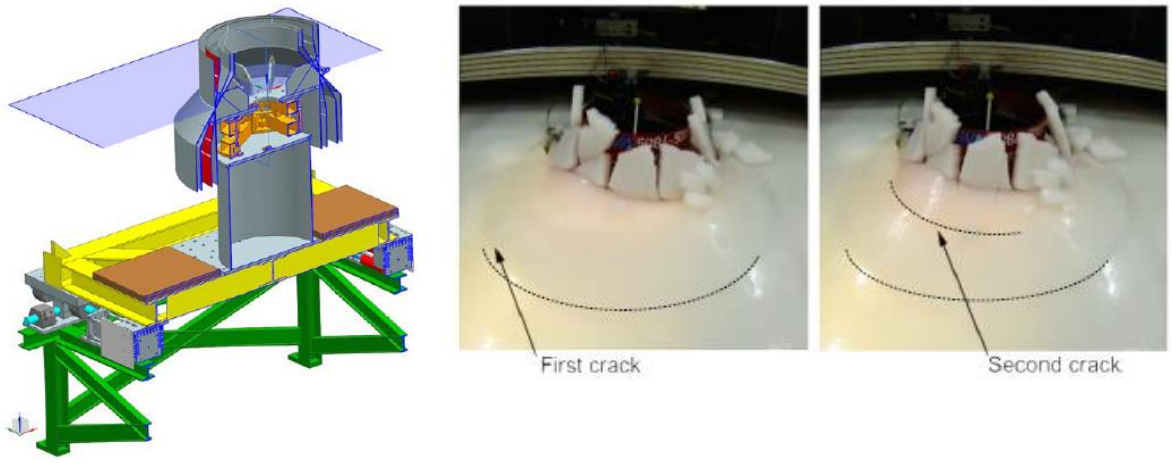

Figure 40. Schematic diagram of the model set-up (left); photographs showing the two-time cracking during upward bending ice failure on the cone (right).

Load and response on the cylindrical reference structure in case of lock-in

Only short events of lock-in have been observed, all interrupted by bending failure, eliminating the chance of persistent lock-in vibrations. However, several short events can be used as reference case to define the worst case scenario. All events show similar high forces and response amplitudes, i.e. 3500 N to 4000 N (model scale) maximum ice load and 4 mm periodic amplitude of oscillation. Figure 41 shows FFT of load and response of a lock-in like event. Next to a frequency close to the natural frequency (3.15 Hz, i.e. 10% lower than natural frequency), the first harmonic is very pronounced in the frequency spectrum of the ice load (Ziemer, et al., 2015).

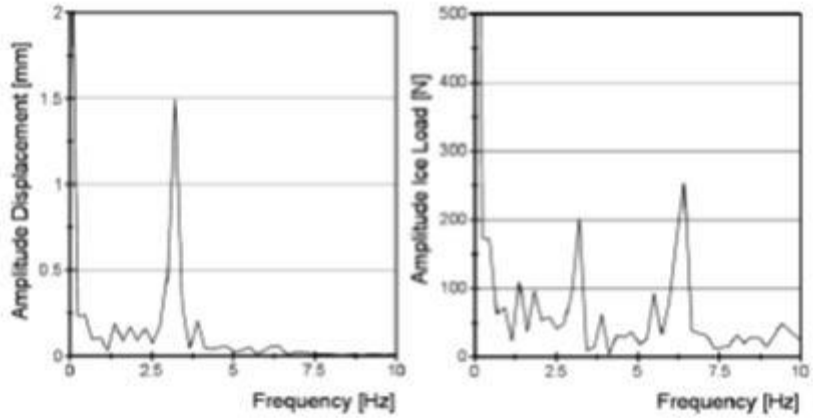

Figure 41. FFT of response (left) and load (right) during lock-in like event of 5 seconds duration (Ziemer, et al.,2015)

EU-Hydralab-Plus project: Loads on Structure and Waves in Ice (LS-WICE)

A multi-group research project was conducted recently under the EU-Hydralab+ Transnational Access project: Loads on Structure and Waves in Ice (LS-WICE). There are three parts to this investigation: (a) ice fracture under wave actions, (b) wave attenuation/dispersion in broken ice covers, and (c) ice-structure interaction under wave conditions. This paper focuses on the wave attenuation/dispersion part of the investigation. A level ice sheet was produced first. The physical and mechanical properties were measured in the Large Ice Model Basin (LIMB) before passing through a range of waves to obtain the attenuation/dispersion relation. Wave measurements were monitored with pressure transducers and ultrasound sensors. The test sequence began with a continuous ice sheet followed by broken ice sheet. The broken ice sheet was produced by cutting the continuous ice sheet into uniform size floes. A range of floe sizes and wave periods were tested (Cheng, et al., 2017; Herman, et al., 2017; Tsarau, et al., 2017). The test program was executed in open water and in 4 ice sheets. A cylindrical structure was stationary anchored in ice sheet no. 4 in order to measure the ice and wave forces acting on the cylinder as shown in Figure 44 (Tsarau, et al., 2017). Each of these tests had different purposes. The open water case was performed to characterize the wave tank behavior and to calibrate all sensors. Ice sheet no. 1 was produced to perform the break-up test. Ice sheets no. 2 and no. 3 were used to test wave attenuation and dispersion under different monochromatic waves. Ice sheet no. 4 was produced to test ice-structure interaction in the presence of a wave field.

Ice fracture under wave actions

The effect of ice floe size relative to wavelength on wave propagation was investigated. Parameters to be determined from these two inputs include the wavelength and the attenuation rate.

A level ice sheet was formed by seeding method first to create a granular layer. Sustained cooling thickened this top layer by columnar growth until the whole sheet reaches about 0.035 m thickness. The Young's modulus, flexural strength, ice thickness, density and salinity were then measured.

A sequence of wave tests with different wave periods was first applied to the intact level ice cover. The intact level ice was then cut longitudinally into six 1.5 m wide strips parallel to the wave tank wall. Transverse cuts were applied to create floes of uniform sizes. Prior to the tests the ice sheet was cut into 6 m long and 1.5 m wide ice floes. After applying a set of wave tests with different periods, these floes were further cut into 3 m, then 1.5 m, and finally 0.5 m floes. Each time a pattern of uniform size floes was produced. Figure 42 shows the floe field for the 6 m case and the 0.5 m case (Cheng et al., 2017).

Figure 42. The regular width of ice floes tested were 1.5 m wide. The length of the floes started with 6 m, as shown in the left side photo and ended with 0.5 m, as shown in the right side photo, both taken just after the cutting prior to the wave tests. The whole ice cover was refrained from spreading by the boom at the leading edge. The first row of the 6 m long floes was broken by waves as evident from the right side photo (Cheng, et al., 2017).

The wave tests included wave periods between 0.9 to 2 s, starting from long wave to minimize the risk of breaking floes. However, the 6 m floes were proven to be too long to keep their integrity. The first row of these floes did break, as can be seen from Figure 42 (right side photo).

A stop-go wave test was performed. Each test run lasted between 80 to 90 s, sufficient for each of the wave tested to travel the entire wave tank and return to ice edge. However, because no beach could perfectly absorb wave energy, to avoid effects from reflection, only a portion of the wave record before any wave reflection will be used for further analysis (Cheng et al., 2017).

Wave attenuation/dispersion in broken ice covers

The test sequence began with a continuous ice sheet followed by broken ice sheet. A few markers were placed on the ice sheet tracking the 3D motion with infrared camera system (Qualisys™ Motion Capture System). Prior to the tests the physical and mechanical properties were measured before passing through a range of waves to obtain the attenuation/dispersion relation. Pressure transducers and ultrasound sensors located at different positions along the ice tank were used to monitor the wave propagation through the ice. The progress of breaking was recorded with cameras placed above as well as sideways from the tank. The measurements consisted of two groups of tests, with a constant wave period in each group. The wave amplitude was increased stepwise, starting from a value too low to break the ice, until a major fragmentation of ice occurred. After each group of tests, the locations of cracks were determined and the floe-size distribution was estimated (Herman et al., 2017).

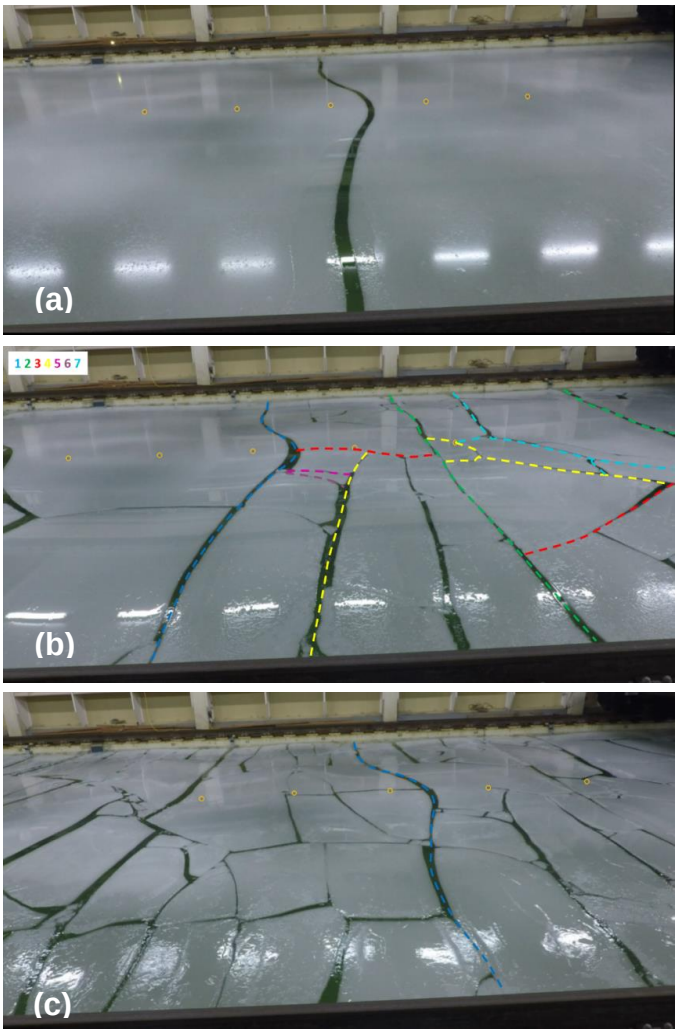

Figure 43. Snapshots of the ice sheet from the GoPro Silver camera after test 1440 (a), 1450 (b) and 1510 (c), after removal of fish-eye effects. The Qualisys markers are highlighted with yellow circles for better visibility. In (b) and (c), the location of the initial crack is marked with a dashed blue line. Additionally in (b), the time sequence of the crack formation in the initial phases of test 1450 is shown with lines of different colors (according to the color code in the upper left corner of the image); (Herman, et al., 2017).

Ice-structure interaction under wave conditions

Another experiment in this project focused on studying combined wave and ice actions on a fixed structure represented by a cylinder with a diameter of 0.69 m. The structure was located approximately in the middle of the ice tank at 43.7m from the wave maker as shown in Figure 44. The ice concentration near the structure was approximately 100%. Apart from the structure and the ice field, Figure 45 shows a number of sensors and video cameras that were used in the tests: 12 pressure sensors and 2 ultrasound sensors to measure wave height; Qualisys cameras and markers to monitor ice deflection; an Inertial Measurement Unit (IMU) to record the accelerations of an ice floe; video cameras on the ceiling, side walls, above the structure and under the water surface to monitor the ice cover and the ice-structure interaction area. A set of load cells that were installed inside the structure and fixed to a rigid carriage was used to measure loads on the structure. As shown in Figure 44 the IMU was installed at the center of an ice floe adjacent to the structure to obtain the response in waves and impact accelerations (Tsarau, et al., 2017).

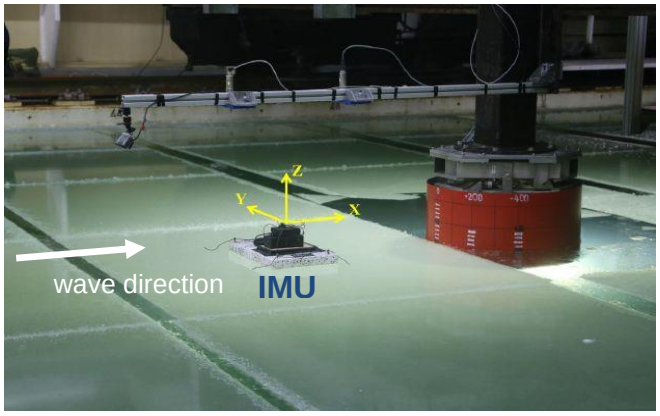

Figure 44. Structure and an adjacent ice floe equipped with an IMU.

The layout of the locations of sensors used in the ice-structure interaction tests is shown in Figure 45.

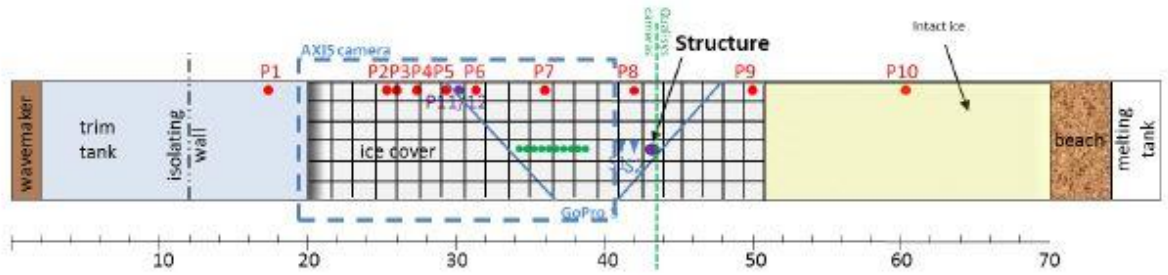

Figure 45. Layout of the wave tank and sensors. P1 –P10 are single pressure sensors, P11/12– double pressure sensor, S1 and S2 – ultrasound sensors, continuous blue lines –fields of view of GoPro camera, dashed blue lines – field of view of the AXIS™ camera, continuous black lines – locations of longitudinal and transverse cuts (i.e., floe boundaries), yellow rectangle – a region, where no transverse cuts were done during the tests, green points – location of the Qualisys™ markers, dashed green line – approximate location of the Qualisys™ cameras and the IMU (Tsarau, et al., 2017).

The global loads from both only waves and combined ice/wave action were measured. Waves with periods T = 1.5 s – 2.0 s and heights 25 mm – 75 mm were used in the tests. Two additional test runs were performed with wave heights H = 100 mm and 200 mm and wave period T =1.6 s; major fractures of the ice floes were observed in these test runs. (Tsarau, et al., 2017).

Among the parameters influencing the impact force, following was identified:

- wave height and period (also wave length for shallow water);
- ice-floe kinematics in waves, including momentum exchange due to floe-floe interaction;
- Interaction area between the structure and the ice floe.

A major difference of this experiment compared to previous experiments on impacts of a wave-driven ice mass on a structure is the utilization of a wave tank fully covered with ice floes instead of considering only one isolated ice mass and a structure. Full ice coverage ensures a better representation of MIZ conditions and allows taking into account floe-floe interactions and the wave dispersion effects in ice-covered water.

CONCLUSIONS

The increase in offshore activities in Arctic regions as well as the further development of icebreaking ships with regard to performance in ice, strength and safety over the past 50 years has stimulated to further develop hydrodynamic test facilities in order to meet the extended requirements. Due to the diversity of the projects, especially in the offshore sector and development of the Northern Sea Route, HSVA responded with the expansion of its facilities. A new type of model has been developed and introduced. Test procedures, measurement technology and data analysis were standardized and extended to simulate complex test scenarios. Increasingly, physical experiments are being performed to validate numerical simulations. Currently, a trend is observed that due to climate change the ice tanks are not only used by commercial clients from shipbuilding and oil industry but more often used for investigations by researchers from universities, because it is possible to model different scenarios under controlled environmental conditions, which is a cost-effective alternative compared to expensive field tests in the Arctic.
Nowadays numerical models are becoming increasingly important in the field of ice engineering and Arctic technology. However numerical simulations always have to be verified. Consequently the execution of physical ice model tests is furthermore essential and the ice testing facilities have to adapt to the future challenges.

ACKNOWLEDGEMENTS

The work described in this publication was partly financially supported by the European Community's Horizon2020 Research and Innovation Programme through the grant to HYDRALAB-PLUS, Contract no. 654110.

REFERENCES

Bonnemaire, B., Lundamo, T., Evers, K.-U., Løset, S., and Jensen, A.,2008. Model Testing of the Arctic Tandem Offloading Terminal Mooring Ice Ridge Loads. *19th IAHR International Symposium on Ice "Using New Technology to Understand Water-Ice Interaction*", Vancouver, British Columbia, Canada, July 6 to 11, 2008.

Bonnemaire, B., Aksnes, V., Lundamo, T., Evers, K.-U., Sveinung Løset, S., and Ravndal, O., 2010. Ice Basin Testing of a Moored Offloading Icebreaker in Variable Ice Drift: Innovations and New Findings. *Proceedings of the HYDRALAB III Joint User Meeting*, Hannover, February 2010.

Cheng, S., Tsarau, A., Li, H., Herman, A., Evers, K.-U., and Shen, H. (2017). Loads on Structure and Waves in Ice (LS-WICE) project, Part 1: Wave attenuation and dispersion in broken ice fields, *Proceedings of the 24th International Conference on Port and Ocean Engineering under Arctic Conditions*, June 11-16, 2017, Busan, Korea

Evers, K.-U. (2016), Modeling ice processes in laboratories and determination of model ice properties, in *Cold Regions Science and Marine Technology* , [Eds. Pat Langhorne, Hayley Shen, Matti Leppäranta, Knut Høyland], in *Encyclopedia of Life Support Systems (EOLSS)*, Developed under the Auspices of the UNESCO, Eolss Publishers, Oxford, UK, [http://www.eolss.net]

Evers, K.-U. and Jochmann, P. (2011). Experiences at HSVA with model testing of moored structures in ice-covered waters, *Proceedings of the 21st International Conference on Port and Ocean Engineering under Arctic Conditions (POAC)*, July 10-14, 2011 Montréal, Canada

Evers, K.-U. and Jochmann, P., (1993) .An Advanced Technique to Improve the Mechanical Properties of Model Ice Developed at the HSVA Ice Tank, *Proceedings of the 12th International Conference on Port and Ocean Engineering under Arctic Conditions (POAC)*, 17- 20 Aug. 1993, Hamburg, Vol. 2, pp. 877-888

Frederking, R. and Häusler, F.U., (1978). The flexural behaviour of ice from *in situ* cantilever beam tests, *Proc. IAHR Symp. on Ice Problems*, Part I, Lulea, Sweden, pp. 197-215.

Haase, A., van der Werff, S. and Jochmann, P., (2012). DYPIC - Dynamic Positioning in Ice: First Phase of Model Testing, *Proceedings of the 31st International Conference on Ocean, Offshore and Arctic Engineering OMAE 2012*, July 1-6, 2012, Rio de Janeiro, Brazil, Paper No. OMAE2012-83455.

Hellmann, J.-H., Rupp, K.-H., Evers, K.-U. and Häusler, F.U., (1992). *Method and devices for forming a sheet of ice for, in particular, tests with ship models or models of marine structures*, Patent No. PCT/EP1992/000305; DE 4106930 A1.

Herman, A., Tsarau, A., Evers, K.-U., Li, H. and Shen, H. (2017). Loads on Structure and Waves in Ice (LS-WICE) project, Part 2: Sea ice breaking by waves, *Proceedings of the 24th International Conference on Port and Ocean Engineering under Arctic Conditions (POAC'17)*, June 11-16, 2017, Busan, Korea

Kim, J.-H. and Choi, K., (2011). Comparison of EG/AD/S and EG/AD model ice properties, *International Journal of Ocean System Engineering* ,1(1) (2011) 32-36
DOI 10.5574/IJOSE.2011.1.1.32

Lee, C.-J., Cho, S.-R., Jeong, S.-Y., Chun, E.-J., (2010). MOERI's Ice Model Test for Korean Icebreaking Research Vessel, *Proc. Intern. Conference and Exhebition on Performance of Ships and Structures in Ice, ICETECH 2010* , September 20-23, 2010, Anchorage, Alaska, USA

Riska, K.(2014). *Factors influencing the power requirement in the Finnish-Swedish Ice Class Rules*, Research Report Finnish Transport Safety Agency - Swedish Maritime Administration, Research Report No. 67, 2014

Sand, B., (2008). *Nonlinear finite element simulations of ice forces on offshore structures*, Doctoral Thesis, Luleå University of Technology, Department of Civil, Mining and Environmental Engineering Division of Structural Engineering

Schwarz, J. *et al*. (1981). Standardized testing methods for measuring mechanical properties of ice, *Cold Regions Science and Technology*, 4 (1981) 245-253 245, Elsevier, Amsterdam - Printed in The Netherlands

Sodhi, D.S., Kato, K., Haynes, F.D. and Hirayama, K. (1982). Determining the Characteristic Length of Model Ice Sheets, *Cold Regions Science and Technology*, 6, 1982, pp.99-104.

Spencer, D.S. and Timco, G.W., (1990). CD Model ice: A process to produce correct density (CD) model ice. *In Proceedings of the IAHR 10th International Symposium on Ice*, August, Espoo, Finland. International Association for Hydraulic Research, vol. 2, p. 745 755.

Sutherland, J. and Evers, K.-U. (editors), (2013). *Foresight study on laboratory modelling of wave and ice loads on coastal and marine structures*, Deliverable D2.3 , EC contract no. 261520, HYDRALAB-IV.

Svec, O.J. and Frederking, R.M.W., (1981). Cantilever beam tests in an ice cover: Influence of plate effects at the root, *Cold Regions Science and Technology* 4(2): 93-101

Tatinclaux, J.C. and Hirayama, K. (1982). Determination of the Flexural Strength and Elastic Modulus of Ice from *In Situ* Cantilever Beam tests, *Cold Regions Science and Technology*, 6, 1982, pp.37-47.

Timco, G.W., (1981). Invited commentary: on the test methods for model ice. *Cold Regions Science and Technology*., 4: 269-274.

Timco, G.W., (1986). EG/AD/S: A New Type of Model Ice for Refrigerated Towing Tanks, *Cold Regions Science and Technology*, 12 (1986) 175-195, Elsevier Science Publishers B.V.,Amsterdam - Printed in The Netherlands

Timco, G.W. and Weeks, W.F. (2010). A review of the engineering properties of sea ice, *Cold Regions Science and Technology* 60 (2010) 107 129

Tsarau, A., Sukhorukov, S., Herman, A., Evers, K.-U., Li, H. and Løset, S. (2017). Loads on Structure and Waves in Ice (LS-WICE) project, Part 3: Ice-structure interaction under wave conditions, *Proceedings of the 24th International Conference on Port and Ocean Engineering under Arctic Conditions (POAC'17)*, June 11-16, 2017, Busan, Korea

Valanto, P. and Schwarz, J., (1999). Eisbrechtechnik in Deutschland, *100 Jahre Schiffbautechnische Gesellschaft*, Berlin-Heidelberg- New York, Springer, 2001, pp 148-156, DOl: 10.1007/978-3-642-93390-5

van der Werff, S. (2012). *Dynamic positioning in Ice – Assessment of hull forces induced by managed ice fields*, TU Delft, Master thesis, June 2012.

van der Werff, S. and Haase, A., (2012). Influence of the Ice Concentration on the Ice Loads on the Hull of a Ship in a Managed Ice Field, *Proceedings of 31st International Conference on Ocean, Offshore and Arctic Engineering OMAE 2012*, July 1-6, 2012, Rio de Janeiro, Brazil, Paper No. OMAE2012-83927.

Ziemer, G., Evers, K.-U. und Voosen, C., 2015. Influence of structural compliance and slope angle on ice loads and dynamic response of conical structures, *Proceedings of the ASME 2015 34th International Conference on Ocean, Offshore and Arctic Engineering OMAE2015*, May 31-June 5, 2015, St. John's, Newfoundland, Canada, [OMAE2015-41769].

Zhang, Q. and van der Werff, S. (2012). Image Processing for the Analysis of an Evolving Broken-Ice Field in Model Testing, *Proceedings of the 31st International Conference on Ocean, Offshore and Arctic Engineering OMAE 2012*, July 1-6, 2012, Rio de Janeiro, Brazil, [OMAE2012-84117].